Joint Particle Filtering of Multiple Maneuvering Targets From Unassociated Measurements

HENK A. P. BLOM
EDWIN A. BLOEM
National Aerospace Laboratory NLR

The problem of maintaining tracks of multiple maneuvering targets from unassociated measurements is formulated as a problem of estimating the hybrid state of a Markov jump linear system from measurements made by a descriptor system with independent, identically distributed (i.i.d.) stochastic coefficients. This characterization is exploited to derive the exact equation for the Bayesian recursive filter, to develop two novel Sampling Importance Resampling (SIR) type particle filters, and to derive approximate Bayesian filters which use for each target one Gaussian per maneuver mode. The two approximate Bayesian filters are a compact and a track-coalescence avoiding version of Interacting Multiple Model Joint Probabilistic Data Association (IMMJPDA). The relation of each of the four novel filter algorithms to the literature is well explained. Through Monte Carlo simulations for a two target example, these four filters are compared to each other and to the approach of using one IMMPDA filter per target track. The Monte Carlo simulation results show that each of the four novel filters clearly outperforms the IMMPDA approach. The results also show under which conditions the IMMJPDA type filters perform close to exact Bayesian filtering, and under which conditions not.

Manuscript received July 7, 2004; revised December 31, 2005 and May 2, 2006.

Refereeing of this contribution was handled by Shozo Mori.

Authors' addesss: National Aerospace Laboratory NLR Amsterdam, The Netherlands, E-mail: (blom@nlr.nl, bloem@nlr.nl).

1557-6418/06/$17.00

1. INTRODUCTION

In the literature approximate Bayesian approaches towards maintaining tracks of multiple maneuvering targets from unassociated measurements have focussed on the development of combinations of Interacting Multiple Model (IMM) and Joint Probabilistic Data Association (JPDA) approaches. Initially, combinations of IMM and JPDA have been developed along two heuristic directions. Bar-Shalom et al. [4] heuristically developed an IMMJPDA-Coupled filter for situations where the measurements of two targets are unresolved during periods of close encounter. The filters of the individual targets are coupled through cross-target-covariance terms. The filtering results obtained have not been very encouraging to continue this heuristic approach. De Feo et al. [20] combined JPDA and a rather crude approximation of IMM, under the name IMMJPDA. The first proper combination of IMM and JPDA was developed by Chen and Tugnait [18]. Focus of this development was on showing that fixed-lag IMMJPDA smoothing performed far better than IMMJPDA filtering at the cost of 3 scans delay. In [9], [10] we used the descriptor system approach [8] to develop a track-coalescence-avoiding version of IMMJPDA (for short IMMJPDA*). Moreover, we showed that both IMMJPDA and IMMJPDA* perform much better than just applying IMMPDA filtering per maintained track. In spite of these developments it remains unclear how IMMJPDA and IMMJPDA* filtering performs in comparison with the exact Bayesian filter.

This motivates us to study the Sampling Importance Resampling (SIR) based Particle Filter (PF) paradigm [21, 28, 43] for maintaining tracks of multiple maneuvering targets from unassociated measurements. During the last decade this paradigm has been recognized as a practical means for approximating an exact Bayesian filter arbitrarily well. This has stimulated the development of a large variety of particle filters (e.g. [1, 22, 38, 42]) that typically outperform established approximate non-linear filtering and target track maintenance approaches such as Extended Kalman Filtering, Probabilistic Data Association (PDA), the Interacting Multiple Model (IMM) algorithm, and their combinations.

The extension of these results to multiple target tracking situations has also received significant attention. Early on it was recognized that the JPDA formalism provided a logical starting point for this development. Gordon [26] developed a SIR-PF version by replacing JPDA's Gaussian density by a density the evolution of which is approximated with help of a SIR particle filter. Avitzour [2] developed a more advanced SIR particle filter by using joint-target particles; we refer to this as SIR joint PF. Karlsson and Gustafsson [30] compared the RMS position errors of a SIR joint PF with those of a JPDA filter for maintaining tracks in an example of two perpendicular crossing targets. For this "easy" example the difference in performance appeared to be small. Salmond et al. [45] showed that a SIR joint PF works well for the initialization of two non-maneuvering targets that start from the same initial position. Gordon et al. [27] developed a SIR joint PF approach for tracking a group of targets, the members of which stay close to each other. Through several complementary studies, efficiency improvements have been developed for these particle filters, e.g. [29, 41, 42, 48]. To track multiple objects for robotic vision, Schultz et al. [46] developed an occlusion extension for SIR PF and showed that this outperformed JPDA on a multi-person tracking problem. Tracking multiple objects with occlusion situations by SIR joint PF for robotic vision has been shown in [33] and [34].

A complementary development in SIR particle filtering is to use sensor measurements at the pixel level as observations. This allows handling the problems of target detection and target tracking in an integrated way, and thus to shortcut the traditional sequence of signal processing first, followed by target detection (thresholding) and then target tracking. The feasibility of a track-before-detect particle filtering approach has been introduced in [15, 44] for a single target. Extensions to multiple targets have been developed in [40] using single target particles, and in [17, 32, 35] using joint particles. For the current paper we assume that track maintenance has to be performed on the basis of detected measurement observations, and that pixel level sensor measurements are not available. Hence, the track-before-detect problem setting goes beyond the scope of the current study.

The aim of this paper is to extend the SIR joint particle filter approach towards track maintenance, to the situation of multiple maneuvering targets and to evaluate for an example how the performance of these particle filters compares with IMMJPDA and IMMJPDA* filtering. This asks for the combination of an SIR joint PF for unassociated measurements with an SIR PF for tracking a suddenly maneuvering target [16, 36, 37]. The basis for this integration is provided by the exact Bayesian filter for this particular problem. We developed such an exact Bayesian characterisation using the descriptor system approach [10, 14]. The current paper extends these results in the sense of incorporating a non-homogeneous false measurement density [39].

The specialty of this exact characterization is that both the mode switching and the data association are performed jointly for all targets and that the false plot density is non-homogeneous. Based on such exact equations, we develop a standard SIR particle filter to evaluate the exact Bayesian equations. A weakness of this standard SIR joint particle filter is that after a resampling step for some of the joint modes there may be hardly any or even no particles left. In theory this can be compensated for by significantly increasing the number of particles. However, a more effective approach is to resample a fixed number of joint particles per joint mode. We refer to this as hybrid SIR joint particle filtering. Through Monte Carlo simulations for a simple example the standard SIR and hybrid SIR joint particle filters are compared with the following three combinations of IMM and PDA:

- An IMMPDA filter, which updates an individual IMM track using MMPDA [25] and implicitly assuming there are no other targets;
- A compact version of IMMJPDA, which we derive in this paper in a systematic way from the exact Bayesian filter equations; and
- The track coalescence avoiding version (IMMJPDA*) of this compact IMMJPDA.

The paper is organized as follows. Section 2 formulates the multi-target track maintenance problem considered. Section 3 embeds this in filtering for a jump linear descriptor system. Section 4 develops an exact Bayesian characterization of the evolution of the conditional density for the state of the multiple targets. Section 5 develops the standard SIR joint particle filter. Section 6 develops the hybrid SIR joint particle filter. Section 7 adopts the IMMJPDA assumptions, and shows the impact on the filter equations relative to those of [18]. Section 8 develops IMMJPDA*. Section 9 illustrates and compares the performance of these filters through Monte Carlo simulation results. As a performance reference we also run single target IMMPDA filters on the same scenario. Finally, Section 10 draws conclusions.

2. MULTITARGET TRACK MAINTENANCE PROBLEM

Consider M targets and assume that the state of the ith target is modelled as a jump linear system:

$$x_t^i = a^i(\theta_t^i)x_{t-1}^i + b^i(\theta_t^i)w_t^i, \qquad i = 1,\ldots,M \tag{1}$$

where x_t^i is the n-vectorial state of the ith target, θ_t^i is the Markovian switching mode of the ith target and assumes values from $\mathbb{M} = \{1,\ldots,N\}$ according to a transition probability matrix Π^i, $a^i(\theta_t^i)$ and $b^i(\theta_t^i)$ are $(n \times n)$- and $(n \times n')$-matrices and w_t^i is a sequence of i.i.d. standard Gaussian variables of dimension n' with w_t^i, w_t^j independent for all $i \neq j$ and w_t^i, (x_0^i,θ_0^i), (x_0^j,θ_0^j) independent for all $i \neq j$. At $t = 0$, the joint density $p_{x_0^i,\theta_0^i}$ is known for each $i \in [1,M]$; typically these are i-variant.

A set of measurements consists of measurements originating from targets and measurements originating from clutter. We assume that a potential measurement originating from target i is also modelled as a jump linear system:

$$z_t^i = h^i(\theta_t^i)x_t^i + g^i(\theta_t^i)v_t^i, \qquad i = 1,\ldots,M \tag{2}$$

where z_t^i is an m-vector, $h^i(\theta_t^i)$ is an $(m \times n)$-matrix and $g^i(\theta_t^i)$ is an $(m \times m')$-matrix, and v_t^i is a sequence of i.i.d. standard Gaussian variables of dimension m' with v_t^i and

v_t^j independent for all $i \neq j$. Moreover v_t^i is independent of x_0^j and w_t^j for all i,j.

Let $x_t \triangleq \text{Col}\{x_t^1, \ldots, x_t^M\}$, $\theta_t \triangleq \text{Col}\{\theta_t^1, \ldots, \theta_t^M\}$, $A(\theta_t) \triangleq \text{Diag}\{a^1(\theta_t^1), \ldots, a^M(\theta_t^M)\}$, $B(\theta_t) \triangleq \text{Diag}\{b^1(\theta_t^1), \ldots, b^M \cdot (\theta_t^M)\}$, and $w_t \triangleq \text{Col}\{w_t^1, \ldots, w_t^M\}$. Then we can model the state of our M targets as follows:

$$x_t = A(\theta_t)x_{t-1} + B(\theta_t)w_t \tag{3}$$

with A and B of size $Mn \times Mn$ and $Mn \times Mn'$ respectively, with $\{\theta_t\}$ assuming values from $\mathbb{M}^M$ according to the transition probability matrix $\Pi = [\Pi_{\eta,\theta}]$. If the M targets switch mode independently of each other, then:

$$\Pi_{\eta,\theta} = \prod_{i=1}^{M} \Pi^i_{\eta^i,\theta^i} \tag{4}$$

for every $\eta \in \mathbb{M}^M$ and $\theta \in \mathbb{M}^M$.

Next with $z_t \triangleq \text{Col}\{z_t^1, \ldots, z_t^M\}$, $H(\theta_t) \triangleq \text{Diag}\{h^1(\theta_t^1), \ldots, h^M(\theta_t^M)\}$, $G(\theta_t) \triangleq \text{Diag}\{g^1(\theta_t^1), \ldots, g^M(\theta_t^M)\}$, and $v_t \triangleq \text{Col}\{v_t^1, \ldots, v_t^M\}$, we obtain:

$$z_t = H(\theta_t)x_t + G(\theta_t)v_t \tag{5}$$

with H and G of size $Mm \times Mn$ and $Mm \times Mm'$ respectively.

We next assume that with a non-zero detection probability, P_{d}^i, target i is indeed observed at moment t. In addition to this there may be false measurements, the density of which is not homogeneous. Similar to [39] we assume that the number of false measurements at moment t, F_t, has a Poisson distribution:

$$\begin{aligned} p_{F_t}(F) &= \frac{(\hat{F}_t)^F}{F!} \exp(-\hat{F}_t), \qquad && F = 0,1,2,\ldots \\ &= 0, && \text{else} \end{aligned} \tag{6a}$$

where $\hat{F}_t$ is the expected number of false measurements. Let f_t denote the column vector of i.i.d. false measurements, then the conditional density of f_t given F_t satisfies:

$$p_{f_t|F_t}(f \mid F) = \prod_{i=1}^{F} p_f(f^i) \tag{6b}$$

where $p_f(\cdot)$ is the (measurable) probability density function of a false measurement. Hence, the local density $\lambda(\cdot)$ of false measurements satisfies:

$$\lambda(f^i) = \hat{F}_t p_f(f^i). \tag{6c}$$

Furthermore we assume that the process $\{F_t, f_t\}$ is a sequence of independent vectors, which are independent of $\{x_t\}$, $\{w_t\}$ and $\{v_t\}$.

At moment $t = 1,2,\ldots,T$ a vector observation y_t is made, the components of which consist of the potential observations z_t^i of the detected targets plus the false measurements $\{F_t, f_t\}$. The multi-target track maintenance problem considered is to estimate x_t, θ_t given observations $Y_t \triangleq \{\text{y}_s; 0 \leq s \leq t\}$ with y_0 representing the initial joint density p_{x_0,θ_0}.

3. STOCHASTIC MODELLING OF OBSERVATION EQUATION

This section characterizes the exact relationship between observation vector y_t and the false and potential observations at moment $t > 0$. For this we largely follow [8]. The measurement vector y_t consists of measurements originating from targets and measurements originating from clutter. Firstly, the relation for measurements originating from targets is identified. Subsequently, the clutter measurements are randomly inserted between the target measurements.

Let $\phi_{i,t} \in \{0,1\}$ be the detection indicator for target i, which assumes the value one with a time invariant probability $P_{\text{d}}^i > 0$, independently of $\phi_{j,t}$, $j \neq i$ and independently of the processes introduced in Section 2. This approach yields the following detection indicator vector ϕ_t of size M:

$$\phi_t \triangleq \text{Col}\{\phi_{1,t}, \ldots, \phi_{M,t}\}.$$

Thus, the number of detected targets is $D_t \triangleq \sum_{i=1}^{M} \phi_{i,t}$. Furthermore, we assume that $\{\phi_t\}$ is a sequence of i.i.d. vectors.

In order to link the detection indicator vector with the measurement model, we introduce the following operator Φ: for an arbitrary vector ϕ' of length M' and having $(0,1)$ valued components, we define $D(\phi') \triangleq \sum_{i=1}^{M'} \phi'_i$ and the operator Φ producing $\Phi(\phi')$ as a $(0,1)$-valued matrix of size $D(\phi') \times M'$ of which the ith row equals the ith non-zero row of $\text{Diag}\{\phi'\}$. Next we define, for $D_t > 0$, a vector that contains all measurements originating from targets in a fixed order

$$\tilde{z}_t \triangleq \mathbf{\Phi}(\phi_t) z_t \qquad \text{where} \qquad \mathbf{\Phi}(\phi_t) \triangleq \Phi(\phi_t) \otimes I_m$$

with I_m a unit-matrix of size m, and $\otimes$ the Kronecker product, i.e.,

$$\begin{bmatrix} a & b \\ c & d \end{bmatrix} \otimes I_m \triangleq \begin{bmatrix} aI_m & \vdots & bI_m \\ & \cdots\cdots & \\ cI_m & \vdots & dI_m \end{bmatrix}.$$

In reality, however, we do not know in which order the targets are observed. Hence, we introduce the stochastic $D_t \times D_t$ permutation matrix χ_t, which is independent of the processes introduced in Section 2 and is conditionally independent of $\{\phi_t\}$ given D_t. We also assume that $\{\chi_t\}$ is a sequence of independent matrices. Hence, for $D_t > 0$,

$$\tilde{\tilde{z}}_t \triangleq \boldsymbol{\chi}_t \tilde{z}_t \qquad \text{where} \qquad \boldsymbol{\chi}_t \triangleq \chi_t \otimes I_m$$

is a vector that contains all measurements originating from targets at moment t in a random order.

Let the random variable L_t be the total number of measurements at moment t. Thus,

$$L_t = D_t + F_t.$$

We next describe the relationship between the potential measurement vector z_t, the false plot vector f_t and the measurement vector $\mathrm{y}_t \triangleq \mathrm{Col}\{\mathrm{y}_{1,t},\ldots,\mathrm{y}_{L_t,t}\}$, where $\mathrm{y}_{i,t}$ denotes the ith m-vectorial measurement at moment t. Because y_t contains a random mixture of D_t target measurements and $L_t - D_t$ false measurements, the relation between z_t and y_t can be characterized by the following pair of equations for the target and false measurements respectively:

$$\begin{aligned}\mathbf{\Phi}(\psi_t)\mathrm{y}_t &= \boldsymbol{\chi}_t\mathbf{\Phi}(\phi_t)z_t && \text{if} \quad D_t > 0\\ &= \{\} && \text{if} \quad D_t = 0 \qquad (7a)\\ \mathbf{\Phi}(\psi_t^*)\mathrm{y}_t &= f_t && \text{if} \quad L_t > D_t\\ &= \{\} && \text{if} \quad L_t = D_t \qquad (7b)\end{aligned}$$

where ψ_t, ψ_t^*, χ_t are explained below.

First we explain the target measurement (7a). This equation has stochastic i.i.d. coefficients $\mathbf{\Phi}(\psi_t)$ and $\boldsymbol{\chi}_t\mathbf{\Phi}(\phi_t)$. The detected target measurements in the observation vector y_t are in random order. Hence, the potential detected measurements of targets need to be randomly mixed. To perform this by a simple matrix multiplication, a sequence of independent stochastic permutation matrices $\{\chi_t\}$ of size $D_t \times D_t$ is defined and assumed to be independent of $\{\phi_t\}$. To take into account the measurement vector size m, χ_t needs to be "inflated" to the proper size of $D_t m$ by means of the Kronecker product with I_m. To this end, $\boldsymbol{\chi}_t \triangleq \chi_t \otimes I_m$ with I_m a unit-matrix of size m, and $\otimes$ the Kronecker product. Hence $\boldsymbol{\chi}_t\mathbf{\Phi}(\phi_t)z_t$ is a column vector of potential detected measurements of targets in random order.

$\psi_t \triangleq \mathrm{Col}\{\psi_{1,t},\ldots,\psi_{L_t,t}\}$ is the target indicator vector, where $\psi_{i,t} \in \{0,1\}$ is a target indicator at moment t for measurement i, which assumes the value one if measurement i belongs to a detected target and zero if measurement i is false. Because there are as many detected targets as target measurements, the following constraint applies:

$$D(\psi_t) = D(\phi_t). \qquad (8)$$

Under this equality constraint, $\{\psi_t\}$ is a sequence of independent vectors that is D_t-conditionally independent of all earlier defined processes.

In order to let ψ_t select the correct measurements by simple matrix multiplication, the matrix operator Φ defined above is used. To take into account the measurement vector size m, $\Phi(\psi_t)$ needs to be "inflated" to the proper size of $D_t m$ by means of the Kronecker product with I_m. To this end, $\mathbf{\Phi}(\psi') \triangleq \Phi(\psi') \otimes I_m$ with I_m a unit-matrix of size m, and $\otimes$ the Kronecker product. Hence $\mathbf{\Phi}(\psi_t)\mathrm{y}_t$ is a column vector that contains all detected target measurements in y_t.

$\psi_t^* \triangleq \mathrm{Col}\{\psi_{1,t}^*,\ldots,\psi_{L_t,t}^*\}$ is a false indicator vector of size L_t with $\psi_{i,t}^* = 1 - \psi_{i,t}$. To select the false measurements by matrix multiplication, the matrix operator Φ is used again. Hence $\mathbf{\Phi}(\psi_t^*)\mathrm{y}_t$ is a column vector that contains all false measurements from y_t.

Finally we develop a characterization for y_t. For this we first verify the following for $L_t > D_t > 0$:

$$\Phi(\psi_t)^T\Phi(\psi_t) + \Phi(\psi_t^*)^T\Phi(\psi_t^*) = I_{L_t \times L_t}.$$

Hence

$$\mathrm{y}_t = [\Phi(\psi_t)^T\Phi(\psi_t) + \Phi(\psi_t^*)^T\Phi(\psi_t^*)]\mathrm{y}_t \qquad \text{if} \quad L_t > D_t > 0.$$

Substituting (7a) and (7b) into this equation yields the following model for the observation vector y_t:

$$\begin{aligned}\mathrm{y}_t &= \mathbf{\Phi}(\psi_t)^T\boldsymbol{\chi}_t\mathbf{\Phi}(\phi_t)z_t + \mathbf{\Phi}(\psi_t^*)^T f_t && \text{if} \quad L_t > D_t > 0\\ &= \mathbf{\Phi}(\psi_t)^T\boldsymbol{\chi}_t\mathbf{\Phi}(\phi_t)z_t && \text{if} \quad L_t = D_t > 0\\ &= \mathbf{\Phi}(\psi_t^*)^T f_t && \text{if} \quad L_t > D_t = 0\\ &= \{\} && \text{if} \quad L_t = 0. \qquad (9)\end{aligned}$$

Together with equations (3), (4), (5) and (6), equation (9) forms a complete characterization of our tracking problem in terms of stochastic difference equations.

EXAMPLE Assume we maintain tracks of five targets ($M = 5$), of which we detect detect and observe four ($D_t = 4$) together with two false measurements ($F_t = 2$), and with:

$$\chi_t = \begin{bmatrix}0&0&0&1\\0&0&1&0\\1&0&0&0\\0&1&0&0\end{bmatrix}, \qquad \begin{aligned}\phi_t &= [1\ 0\ 1\ 1\ 1]^T\\ \psi_t &= [1\ 1\ 0\ 1\ 1\ 0]^T\end{aligned}$$

i.e., the 2nd target is not detected, and the 3rd and 6th measurements are false. This implies:

$$\Phi(\phi_t) = \begin{bmatrix}1&0&0&0&0\\0&0&1&0&0\\0&0&0&1&0\\0&0&0&0&1\end{bmatrix}$$

$$\Phi(\psi_t) = \begin{bmatrix}1&0&0&0&0&0\\0&1&0&0&0&0\\0&0&0&1&0&0\\0&0&0&0&1&0\end{bmatrix}$$

$$\Phi(\psi_t^*) = \begin{bmatrix}0&0&1&0&0&0\\0&0&0&0&0&1\end{bmatrix}$$

$$\chi_t \Phi(\phi_t) = \begin{bmatrix} 0 & 0 & 0 & 0 & 1 \\ 0 & 0 & 0 & 1 & 0 \\ 1 & 0 & 0 & 0 & 0 \\ 0 & 0 & 1 & 0 & 0 \end{bmatrix}$$

$$\mathbf{\Phi}(\psi_t)^T \boldsymbol{\chi}_t \mathbf{\Phi}(\phi_t) z_t = [z_{5,t}\ \ z_{4,t}\ \ 0\ \ z_{1,t}\ \ z_{3,t}\ \ 0]^T$$

$$\mathbf{\Phi}(\psi_t^*)^T f_t = [0\ \ 0\ \ f_{1,t}\ \ 0\ \ 0\ \ f_{2,t}]^T.$$

Substituting this in (9) yields:

$$\mathrm{y}_t = [z_{5,t}\ \ z_{4,t}\ \ f_{1,t}\ \ z_{1,t}\ \ z_{3,t}\ \ f_{2,t}]^T.$$

4. EXACT FILTER EQUATIONS

In this section a Bayesian characterization of the conditional density $p_{x_t,\theta_t|Y_t}(x,\theta)$ is given where Y_t denotes the σ-algebra generated by measurements y_t up to and including moment t. Subsequently, characterizations are developed for the mode probabilities and the mode conditional means and covariances.

First we introduce an auxiliary indicator matrix process $\tilde{\chi}_t$ of size $D_t \times L_t$, as follows:

$$\tilde{\chi}_t \stackrel{\Delta}{=} \chi_t^T \Phi(\psi_t) \qquad \text{if} \quad D_t > 0. \tag{10}$$

Pre-multiplying the left- and right hand terms in (9) with $\tilde{\boldsymbol{\chi}}_t = \tilde{\chi}_t \otimes I_m$ and subsequent straightforward evaluation yields:

$$\tilde{\boldsymbol{\chi}}_t \mathrm{y}_t = \mathbf{\Phi}(\phi_t) H(\theta_t) x_t + \mathbf{\Phi}(\phi_t) G(\theta_t) v_t \qquad \text{if} \quad D_t > 0 \tag{11}$$

where the size of $\tilde{\boldsymbol{\chi}}_t$ is $D_t m \times L_t m$ and the size of $\mathbf{\Phi}(\phi_t)$ is $D_t m \times Mm$.

Notice that (11) is a linear Gaussian descriptor system [19] with stochastic i.i.d. coefficients $\tilde{\boldsymbol{\chi}}_t$ and $\mathbf{\Phi}(\phi_t)$ and Markovian switching coefficients $H(\theta_t)$ and $G(\theta_t)$.

From (11), it follows that for $D_t > 0$ all relevant associations and permutations can be covered by $(\phi_t, \tilde{\chi}_t)$-hypotheses. We extend this to $D_t = 0$ by adding the combination $\phi_t = \{0\}^M$ and $\tilde{\chi}_t = \{\ \}^{L_t}$. Hence, through defining the weights

$$\beta_t(\phi, \tilde{\chi}, \theta) \stackrel{\Delta}{=} \mathrm{Prob}\{\phi_t = \phi, \tilde{\chi}_t = \tilde{\chi}, \theta_t = \theta \mid Y_t\}$$

the law of total probability yields:

$$p_{x_t,\theta_t|Y_t}(x,\theta) = \sum_{\tilde{\chi},\phi} \beta_t(\phi,\tilde{\chi},\theta) p_{x_t|\theta_t,\phi_t,\tilde{\chi}_t,Y_t}(x \mid \theta,\phi,\tilde{\chi}). \tag{12}$$

And thus, our problem is to characterize the terms in the last summation. This problem is solved in two steps, the first of which is the following Proposition.

PROPOSITION 1 *For any $\phi \in \{0,1\}^M$, such that $D(\phi) \stackrel{\Delta}{=} \sum_{i=1}^M \phi_i \le L_t$, and any $\tilde{\chi}_t$ matrix realization $\tilde{\chi}$ of size $D(\phi) \times L_t$, the following holds true:*

$$p_{x_t|\theta_t,\phi_t,\tilde{\chi}_t,Y_t}(x \mid \theta,\phi,\tilde{\chi}) = \frac{p_{\tilde{z}_t|x_t,\theta_t,\phi_t}(\tilde{\boldsymbol{\chi}}\mathrm{y}_t \mid x,\theta,\phi) \cdot p_{x_t|\theta_t,Y_{t-1}}(x \mid \theta)}{F_t(\phi,\tilde{\chi},\theta)} \tag{13}$$

$$\beta_t(\phi,\tilde{\chi},\theta) = F_t(\phi,\tilde{\chi},\theta) \cdot \prod_{j=1}^{L_t - D(\phi)} \lambda([\Phi(1_{L_t} - \tilde{\chi}^T\tilde{\chi}1_{L_t})\mathrm{y}_t]_j) \cdot \prod_{i=1}^{M}[(1-P_d^i)^{(1-\phi_i)}(P_d^i)^{\phi_i}] \cdot p_{\theta_t|Y_{t-1}}(\theta)/c_t \tag{14}$$

where $\tilde{\boldsymbol{\chi}} \stackrel{\Delta}{=} \tilde{\chi} \otimes I_m$, $1_{L_t} = [1,\ldots,1]^T$ is an L_t vector with 1-valued elements and $F_t(\phi,\tilde{\chi},\theta)$ and c_t are such that they normalize $p_{x_t|\theta_t,\phi_t,\tilde{\chi}_t,Y_t}(x \mid \theta,\phi,\tilde{\chi})$ and $\beta_t(\phi,\tilde{\chi},\theta)$ respectively.

PROOF See Appendix A.

The next step starts with substituting (13) and (14) into (12), which yields:

$$p_{x_t,\theta_t|Y_t}(x,\theta) = \sum_{\tilde{\chi},\phi}\left[\frac{p_{\tilde{z}_t|x_t,\theta_t,\phi_t}(\tilde{\boldsymbol{\chi}}\mathrm{y}_t \mid x,\theta,\phi) \cdot p_{x_t|\theta_t,Y_{t-1}}(x \mid \theta)}{F_t(\phi,\tilde{\chi},\theta)} \cdot F_t(\phi,\tilde{\chi},\theta) \cdot \prod_{j=1}^{L_t-D(\phi)} \lambda([\Phi(1_{L_t} - \tilde{\chi}^T\tilde{\chi}1_{L_t})\mathrm{y}_t]_j) \cdot \prod_{i=1}^{M}[(1-P_\mathrm{d}^i)^{(1-\phi_i)}(P_\mathrm{d}^i)^{\phi_i}]\right] \cdot p_{\theta_t|Y_{t-1}}(\theta)/c_t.$$

Simplifying this and rearranging terms yields:

$$p_{x_t,\theta_t|Y_t}(x,\theta) = \sum_{\tilde{\chi},\phi}\left[p_{\tilde{z}_t|x_t,\theta_t,\phi_t}(\tilde{\boldsymbol{\chi}}\mathrm{y}_t \mid x,\theta,\phi) \cdot p_{x_t,\theta_t|Y_{t-1}}(x,\theta) \cdot \prod_{j=1}^{L_t-D(\phi)} \lambda([\Phi(1_{L_t} - \tilde{\chi}^T\tilde{\chi}1_{L_t})\mathrm{y}_t]_j) \cdot \prod_{i=1}^{M}[(1-P_\mathrm{d}^i)^{(1-\phi_i)}(P_\mathrm{d}^i)^{\phi_i}]/c_t\right] \tag{15}$$

with

$$p_{\tilde{z}_t|x_t,\theta_t,\phi_t}(\tilde{z} \mid x,\theta,\phi) = N\{\tilde{z}; \mathbf{\Phi}(\phi)H(\theta)x, \mathbf{\Phi}(\phi)G(\theta)G(\theta)^T\mathbf{\Phi}(\phi)^T\}. \tag{16}$$

Define $\tilde{F}_t(\phi,\tilde{\chi},x,\theta) \stackrel{\Delta}{=} p_{\tilde{z}_t|x_t,\theta_t,\phi_t}(\tilde{\chi}\mathrm{y}_t \mid x,\theta,\phi)$. Hence from (16) we get:

$$\tilde{F}_t(\phi,\tilde{\chi},x,\theta) = [(2\pi)^{mD(\phi)}\mathrm{Det}\{\tilde{Q}_t(\phi,\theta)\}]^{-1/2} \cdot \exp\{-\tfrac{1}{2}\tilde{\nu}_t^T(\phi,\tilde{\chi},x,\theta)\tilde{Q}_t(\phi,\theta)^{-1}\tilde{\nu}_t(\phi,\tilde{\chi},x,\theta)\}. \quad (17)$$

where

$$\tilde{\nu}_t(\phi,\tilde{\chi},x,\theta) \stackrel{\Delta}{=} \tilde{\chi}\mathrm{y}_t - \Phi(\phi)H(\theta)x$$

$$\tilde{Q}_t(\phi,\theta) \stackrel{\Delta}{=} \Phi(\phi)(G(\theta)G(\theta)^T)\Phi(\phi)^T.$$

Substituting (17) into (15) and rearranging terms yields

$$p_{x_t,\theta_t|Y_t}(x,\theta) = \frac{1}{c_t}\sum_{\tilde{\chi},\phi}\left[\tilde{F}_t(\phi,\tilde{\chi},x,\theta)\cdot\prod_{j=1}^{L_t-D(\phi)}\lambda([\Phi(1_{L_t}-\tilde{\chi}^T\tilde{\chi}1_{L_t})\mathrm{y}_t]_j) \cdot\prod_{i=1}^{M}[(1-P_\mathrm{d}^i)^{(1-\phi_i)}(P_\mathrm{d}^i)^{\phi_i}]\right]\cdot p_{x_t,\theta_t|Y_{t-1}}(x,\theta). \quad (18)$$

THEOREM 1 *For any $\phi\in\{0,1\}^M$, such that $D(\phi)\stackrel{\Delta}{=}\sum_{i=1}^M \phi_i \le L_t$, the following recursive equation holds true for the conditional density $p_{x_t,\theta_t|Y_t}(x,\theta)$:*

$$p_{x_t,\theta_t|Y_t}(x,\theta) = \frac{1}{c_t}\sum_{\phi\in\{0,1\}^M}\left[\prod_{i=1}^{M}[(1-P_\mathrm{d}^i)^{(1-\phi_i)}(P_\mathrm{d}^i)^{\phi_i}] \cdot\sum_{\tilde{\chi}}N_{mD(\phi)}\{\tilde{\chi}\mathrm{y}_t;\Phi(\phi)H(\theta)x,\Phi(\phi)G(\theta)G(\theta)^T\Phi(\phi)^T\} \cdot\prod_{j=1}^{L_t-D(\phi)}\lambda([\Phi(1_{L_t}-\tilde{\chi}^T\tilde{\chi}1_{L_t})\mathrm{y}_t]_j)\right] \cdot\int_{\mathbb{R}^{Mn}}N_{Mn}\{x;A(\theta)x',B(\theta)B(\theta)^T\} \cdot\sum_{\eta\in\mathbb{M}^M}[\Pi_{\eta\theta}p_{x_{t-1},\theta_{t-1}|Y_{t-1}}(x',\eta)]dx' \quad (19)$$

with normalization c_t, $N_K\{\cdot;\bar{x},\bar{p}\}$ a K-dimensional Gaussian with mean $\bar{x}$ and covariance $\bar{P}$, and the 2nd sum running over all $\tilde{\chi}=\chi\Phi(\psi)$ with χ a $D(\phi)\times D(\phi)$ permutation matrix and $\psi\in\{0,1\}^{L_t}$ such that $D(\psi)=D(\phi)$.

PROOF IMM's basic derivation [38, App. A] yields:

$$p_{x_t,\theta_t|Y_{t-1}}(x,\theta) = \int_{\mathbb{R}^{Mn}}N_{Mn}\{x;A(\theta)x',B(\theta)B(\theta)^T\} \cdot\sum_{\eta\in\{1,\ldots,N\}^M}[\Pi_{\eta\theta}p_{x_{t-1},\theta_{t-1}|Y_{t-1}}(x',\eta)]dx'. \quad (20)$$

Substituting (17) and (20) in (18) and rearranging the summation over $\tilde{\chi}$ yields (19).

Equation (19) is a recursive equation for the exact Bayesian solution for tracking multiple targets from possibly false and missing measurements. From (19) it follows that if the initial density is a Gaussian mixture, then the exact conditional density solution of recursive equation (19) is a Gaussian mixture, the number of Gaussians increasing exponentially with time.

REMARK 1 For jump-linear systems such recursive filter equations have been characterized by [23], and for jump-non-linear systems by [16], [3]. In [14] we provide a version of Theorem 1 under the assumption that λ is homogeneous.

REMARK 2 Proposition 1 and Theorem 1 also apply when the initial densities are permutation symmetric over the targets, i.e. a situation studied by [32].

5. SIR JOINT PARTICLE FILTER

In this section a SIR joint particle filter of the exact filter characterization of Theorem 1 is developed. In this SIR joint PF a particle is defined as a triplet (μ_j,x_j,θ_j), $\mu_j\in[0,1]$, $x_j\in\mathbb{R}^{Mn}$, $\theta_j\in\mathbb{M}^M$, $j\in[1,S]$. One filter cycle consists of the following steps:

- *SIR joint particle filter Step 0:* Initiation.
  Each filter cycle starts with a set of S joint particles in $[0,1]\times\mathbb{R}^{Mn}\times\mathbb{M}^M$, i.e.:

  $$\{(\mu_{j,t-1}=1/S,x_{j,t-1},\theta_{j,t-1});\ j\in[1,S]\}$$

  with, for $t=0$, $\theta_{j,0}$ and $x_{j,0}$ independently drawn from $p_{\theta_0}(\cdot)$ and $p_{x_0|\theta_0}(\cdot\mid\theta_{j,0})$ respectively for each $j\in[1,S]$.
- *SIR joint particle filter Step 1:* Joint mode switching.
  Determine the new joint mode per joint particle ($\mu_{j,t-1}$ and $x_{j,t-1}$ are not changed)

  $$\{(\mu_{j,t-1},x_{j,t-1},\bar{\theta}_{j,t});\ j\in[1,S]\}$$

  by generating for each joint particle a new value $\bar{\theta}_{j,t}$ according to the transition probabilities:

  $$\mathrm{Prob}\{\bar{\theta}_{j,t}=\bar{\theta}\mid\theta_{j,t-1}=\theta\}=\Pi_{\theta,\bar{\theta}}. \quad (21)$$
- *SIR joint particle filter Step 2:* Prediction.
  Determine the new state per joint particle (the weights $\mu_{j,t-1}$ are not changed)

  $$\{(\mu_{j,t-1},\bar{x}_{j,t},\bar{\theta}_{j,t});\ j\in[1,S]\}$$

  by running for each particle a Monte Carlo simulation from $(t-1)$ to t according to the model

  $$\bar{x}_{j,t}=A(\bar{\theta}_{j,t})x_{j,t-1}+B(\bar{\theta}_{j,t})w_{j,t-1}. \quad (22)$$
- *SIR joint particle filter Step 3:* Measurement update.
  Determine new weight per joint particle, i.e.

  $$\{(\bar{\mu}_{j,t},\bar{x}_{j,t},\bar{\theta}_{j,t});\ j\in[1,S]\}$$

with, for the new weights, using (17) and (18):

$$\bar{\mu}_{j,t} = \mu_{j,t-1} \cdot \frac{1}{c_t} \sum_{\tilde{\chi},\phi} \Bigg[\tilde{F}_t(\phi,\tilde{\chi},\bar{x}_{j,t},\bar{\theta}_{j,t}) \cdot \prod_{i=1}^{L_t - D(\phi)} \lambda([\Phi(1_{L_t} - \tilde{\chi}^T \tilde{\chi} 1_{L_t}) \mathrm{y}_t]_i) \cdot \prod_{i=1}^{M} [(1-P_\mathrm{d}^i)^{(1-\phi_i)} (P_\mathrm{d}^i)^{\phi_i}] \Bigg] \quad (23)$$

where

$$\tilde{F}_t(\phi,\tilde{\chi},x,\theta) = [(2\pi)^{mD(\phi)} \mathrm{Det}\{\tilde{Q}_t(\phi,\theta)\}]^{-1/2} \cdot \exp\{-\tfrac{1}{2}\tilde{\nu}_t^T(\phi,\tilde{\chi},x,\theta)\tilde{Q}_t(\phi,\theta)^{-1}\tilde{\nu}_t(\phi,\tilde{\chi},x,\theta)\} \quad (24)$$

with

$$\tilde{\nu}_t(\phi,\tilde{\chi},x,\theta) \stackrel{\Delta}{=} \tilde{\chi}\mathrm{y}_t - \Phi(\phi)H(\theta)x$$

$$\tilde{Q}_t(\phi,\theta) \stackrel{\Delta}{=} \Phi(\phi)(G(\theta)G(\theta)^T)\Phi(\phi)^T$$

and c_t a normalizing constant such that

$$\sum_{j=1}^{S} \bar{\mu}_{j,t} = 1$$

- *SIR joint particle filter Step 4:* MMSE output equations:

$$\hat{\gamma}_t(\theta) = \sum_{j=1}^{S} \bar{\mu}_{j,t} 1_{\bar{\theta}_{j,t}}(\theta)$$

$$\hat{x}_t(\theta) = \sum_{j=1}^{S} \bar{\mu}_{j,t} \bar{x}_{j,t} 1_{\bar{\theta}_{j,t}}(\theta)$$

$$\hat{P}_t(\theta) = \sum_{j=1}^{S} \bar{\mu}_{j,t} [\bar{x}_{j,t} - \hat{x}_t(\theta)][\bar{x}_{j,t} - \hat{x}_t(\theta)]^T 1_{\bar{\theta}_{j,t}}(\theta)$$

$$\hat{x}_t = \sum_{\theta \in \mathbb{M}^M} \hat{\gamma}(\theta)\hat{x}_t(\theta)$$

$$\hat{P}_t = \sum_{\theta \in \mathbb{M}^M} \hat{\gamma}(\theta)[\hat{P}_t(\theta) + [\hat{x}_t(\theta) - \hat{x}_t][\hat{x}_t(\theta) - \hat{x}_t]^T]$$

- *SIR joint particle filter Step 5:* Resampling. Generate the new set of joint particles

$$\{(\mu_{j,t} = 1/S, x_{j,t}, \theta_{j,t});\ j \in [1,S]\}$$

with $\theta_{j,t}$ and $x_{j,t}$ the jth of the S samples drawn independently from the joint particle spanned conditional densities for θ_t given y_t and for x_t given Y_t and $\theta_t = \theta_t^j$:

$$p_{\theta_t|Y_t}(\theta) \approx \hat{\gamma}_t(\theta)$$

$$p_{x_t|\theta_t,Y_t}(\cdot \mid \theta_{j,t}) \approx \sum_{l=1}^{S} \bar{\mu}_t^l 1_{\bar{\theta}_{l,t}}(\theta_{j,t}) \delta_{\bar{x}_{l,t}}(\cdot).$$

In the next section we modify the enumeration of the particles and adopt the particle resampling Step 5.

6. HYBRID SIR JOINT PARTICLE FILTER

In this section a hybrid SIR joint particle filter of the exact filter characterization of Theorem 1 is developed. The difference with the SIR joint particle filter is that we now resample a fixed number of joint particles per joint mode. A joint particle is defined as a triplet $(\mu^{\theta,j}, x^{\theta,j}, \theta)$, $\mu^{\theta,j} \in [0,1]$, $x^{\theta,j} \in \mathbb{R}^{Mn}$, $\theta \in \mathbb{M}^M$, $j \in [1,S']$. One cycle of this hybrid SIR joint particle filter consists of the following steps:

- *Hybrid SIR joint particle filter Step 0:* Initiation. Each filter cycle starts with a set of $S = NS'$ joint particles in $[0,1] \times \mathbb{R}^{Mn} \times \mathbb{M}^M$, i.e.:

$$\{(\mu_{t-1}^{\theta,j}, x_{t-1}^{\theta,j}, \theta_{t-1}^{\theta,j} = \theta);\ j \in [1,S'],\ \theta \in \mathbb{M}^M\}$$

with, for $t = 0$, $\mu_0^{\theta,j} = p_{\theta_0}(\theta)/S'$, and $x_0^{\theta,j}$ independently drawn from $p_{x_0|\theta_0}(\cdot \mid \theta)$ for each $j \in 1,\ldots,S'$.

- *Hybrid SIR joint particle filter Step 1:* Mode switching.
Determine the new mode per particle ($\mu_{t-1}^{\theta,j}$ and $x_{t-1}^{\theta,j}$ are not changed)

$$\{(\mu_{t-1}^{\theta,j}, x_{t-1}^{\theta,j}, \bar{\theta}_t^{\theta,j});\ j \in [1,S'],\ \theta \in \mathbb{M}^M\}$$

by generating for each joint particle a new value $\bar{\theta}_t^{\theta,j}$ according to the model

$$\mathrm{Prob}\{\bar{\theta}_t^{\theta,j} = \bar{\theta} \mid \theta_{t-1}^{\theta,j} = \theta\} = \Pi_{\theta,\bar{\theta}}. \quad (25)$$

- *Hybrid SIR joint particle filter Step 2:* Prediction. Determine the new state per joint particle (the weights $\mu_{t-1}^{\theta,j}$ are not changed)

$$\{(\mu_{t-1}^{\theta,j}, \bar{x}_t^{\theta,j}, \bar{\theta}_t^{\theta,j});\ j \in [1,S'],\ \theta \in \mathbb{M}^M\}$$

by running for each particle a Monte Carlo simulation from $(t-1)$ to t according to the model

$$\bar{x}_t^{\theta,j} = A(\bar{\theta}_t^{\theta,j})x_{t-1}^{\theta,j} + B(\bar{\theta}_t^{\theta,j})w_{t-1}. \quad (26)$$

- *Hybrid SIR joint particle filter Step 3:* Measurement update.
Determine new weight per joint particle, i.e.

$$\{(\bar{\mu}_t^{\theta,j}, \bar{x}_t^{\theta,j}, \bar{\theta}_t^{\theta,j});\ j \in [1,S'],\ \theta \in \mathbb{M}^M\}$$

with for the new weights, using (17) and (18):

$$\bar{\mu}_t^{\theta,j} = \mu_{t-1}^{\theta,j} \cdot \frac{1}{c_t} \sum_{\tilde{\chi},\phi} \Bigg[\tilde{F}_t(\phi,\tilde{\chi},\bar{x}_t^{\theta,j},\bar{\theta}_t^{\theta,j}) \cdot \prod_{i=1}^{L_t - D(\phi)} \lambda([\Phi(1_{L_t} - \tilde{\chi}^T \tilde{\chi} 1_{L_t}) \mathrm{y}_t]_i) \cdot \prod_{i=1}^{M} [(1-P_\mathrm{d}^i)^{(1-\phi_i)} (P_\mathrm{d}^i)^{\phi_i}] \Bigg] \quad (27)$$

where

$$\tilde{F}_t(\phi,\tilde{\chi},x,\theta) = [(2\pi)^{mD(\phi)}\mathrm{Det}\{\tilde{Q}_t(\phi,\theta)\}]^{-1/2} \cdot \exp\{-\tfrac{1}{2}\tilde{\nu}_t^T(\phi,\tilde{\chi},x,\theta)\tilde{Q}_t(\phi,\theta)^{-1}\tilde{\nu}_t(\phi,\tilde{\chi},x,\theta)\} \tag{28}$$

with

$$\tilde{\nu}_t(\phi,\tilde{\chi},x,\theta) \triangleq \tilde{\chi}\mathrm{y}_t - \Phi(\phi)H(\theta)x$$

$$\tilde{Q}_t(\phi,\theta) \triangleq \Phi(\phi)(G(\theta)G(\theta)^T)\Phi(\phi)^T$$

and c_t a normalizing constant such that

$$\sum_{\theta\in\mathbb{M}^M}\sum_{j=1}^{S'}\bar{\mu}_t^{\theta,j} = 1.$$

- *Hybrid SIR joint particle filter Step 4:* MMSE output equations:

$$\hat{\gamma}_t(\theta) = \sum_{\eta\in\mathbb{M}^M}\sum_{j=1}^{S'}\bar{\mu}_t^{\eta,j}1_{\bar{\theta}_t^{\eta,j}}(\theta)$$

$$\hat{x}_t(\theta) = \sum_{\eta\in\mathbb{M}^M}\sum_{j=1}^{S'}\bar{\mu}_t^{\eta,j}\bar{x}_t^{\eta,j}1_{\bar{\theta}_t^{\eta,j}}(\theta)$$

$$\hat{P}_t(\theta) = \sum_{\eta\in\mathbb{M}^M}\sum_{j=1}^{S'}\bar{\mu}_t^{\eta,j}[\bar{x}_t^{\eta,j} - \hat{x}_t(\theta)][\bar{x}_t^{\eta,j} - \hat{x}_t(\theta)]^T 1_{\bar{\theta}_t^{\eta,j}}(\theta)$$

$$\hat{x}_t = \sum_{\theta\in\mathbb{M}^M}\hat{\gamma}(\theta)\hat{x}_t(\theta)$$

$$\hat{P}_t = \sum_{\theta\in\mathbb{M}^M}\hat{\gamma}(\theta)[\hat{P}_t(\theta) + [\hat{x}_t(\theta)-\hat{x}_t][\hat{x}_t(\theta)-\hat{x}_t]^T].$$

- *Hybrid SIR joint particle filter Step 5:* Resampling per mode.
  Generate the new set of joint particles

$$\{(\mu_t^{\theta,j} = \hat{\gamma}_t(\theta)/S', x_t^{\theta,j}, \theta_t^{\theta,j} = \theta);\ j\in[1,S'],\ \theta\in\mathbb{M}^M\}$$

with $x_t^{\theta,j}$ the jth of the S' samples drawn independently from the particle spanned conditional density for x_t given Y_t and $\theta_t = \theta$:

$$p_{x_t|\theta_t,Y_t}(\cdot\mid\theta) \approx \sum_{\eta\in\mathbb{M}^M}\sum_{l=1}^{S'}\bar{\mu}_t^{\eta,l}1_{\bar{\theta}_t^{\eta,l}}(\theta)\delta_{\bar{x}_t^{\eta,l}}(x).$$

For homogeneous λ, this hybrid SIR joint particle filter has been introduced in [11] under the name Joint IMMPDA particle filter.

7. IMMJPDA ASSUMPTIONS

The assumptions that are underlying to the IMMJPDA of [18] are:

C1) $p_{\theta_t|Y_{t-1}}(\theta) = \prod_{i=1}^M p_{\theta_t^i|Y_{t-1}}(\theta^i)$;

C2) $p_{x_t|\theta_t,Y_{t-1}}(x\mid\theta) = \prod_{i=1}^M p_{x_t^i|\theta_t^i,Y_{t-1}}(x^i\mid\theta^i)$;

C3) $p_{x_t^i|\theta_t^i,Y_{t-1}}(x^i\mid\theta^i)$ is Gaussian with mean $\bar{x}_t^i(\theta^i)$ and covariance $\bar{P}_t^i(\theta^i)$.

Application of these assumptions, to the exact equations of Proposition 1 yields the following theorem.

THEOREM 2 *Assume* C1, C2 *and* C3 *are satisfied. Then* $\beta_t(\phi,\tilde{\chi},\theta)$ *of Proposition* 1 *satisfies:*

$$\beta_t(\phi,\tilde{\chi},\theta) = \left[\prod_{i=1}^{L_t-D(\phi)}\lambda([\Phi(1_{L_t} - \tilde{\chi}^T\tilde{\chi}1_{L_t})\mathrm{y}_t]_i)\right] \cdot \prod_{i=1}^{M}[f_t^i(\phi,\tilde{\chi},\theta^i)(1-P_\mathrm{d}^i)^{(1-\phi_i)}(P_\mathrm{d}^i)^{\phi_i}\cdot p_{\theta_t^i|Y_{t-1}}(\theta^i)]/c_t \tag{29}$$

with, for $\phi^i = 0$*:* $f_t^i(\phi,\tilde{\chi},\theta^i) = 1$*, and for* $\phi^i = 1$*:*

$$f_t^i(\phi,\tilde{\chi},\theta^i) = [(2\pi)^m\mathrm{Det}\{\bar{Q}_t^i(\theta^i)\}]^{-\phi_i/2} \cdot \exp\left\{-\frac{1}{2}\sum_{k=1}^{L_t}([\Phi(\phi)^T]_{i*}\tilde{\chi}_{*k}\nu_t^{ik}(\theta^i)^T[\bar{Q}_t^i(\theta^i)]^{-1}\nu_t^{ik}(\theta^i))\right\} \tag{30a}$$

$$\nu_t^{ik}(\theta^i) = \mathrm{y}_t^k - h^i(\theta^i)\bar{x}_t^i(\theta^i) \tag{30b}$$

$$\bar{Q}_t^i(\theta^i) = h^i(\theta^i)\bar{P}_t^i(\theta^i)h^i(\theta^i)^T + g^i(\theta^i)g^i(\theta^i)^T \tag{30c}$$

where $[\Phi(\phi)^T]_{i*}$ *and* $\tilde{\chi}_{*k}$ *are the ith row and kth column of* $\Phi(\phi)^T$ *and* $\tilde{\chi}$*, respectively. Moreover,* $p_{x_t^i|\theta_t^i,Y_t}(x^i\mid\theta^i)$*,* $i\in[1,M]$*, is a Gaussian mixture, while its overall mean* $\hat{x}_t^i(\theta^i)$ *and its overall covariance* $\hat{P}_t^i(\theta^i)$ *satisfy:*

$$p_{\theta_t^i|Y_t}(\theta^i) = \sum_{\substack{\phi,\tilde{\chi},\eta\\ \eta^i=\theta^i}}\beta_t(\phi,\tilde{\chi},\eta) \tag{31a}$$

$$\hat{x}_t^i(\theta^i) = \bar{x}_t^i(\theta^i) + W_t^i(\theta^i)\left(\sum_{k=1}^{L_t}\beta_t^{ik}(\theta^i)\nu_t^{ik}(\theta^i)\right) \tag{31b}$$

$$\hat{P}_t^i(\theta^i) = \bar{P}_t^i(\theta^i) - W_t^i(\theta^i)h^i(\theta^i)\bar{P}_t^i(\theta^i)\left(\sum_{k=1}^{L_t}\beta_t^{ik}(\theta^i)\right) + W_t^i(\theta^i)\left(\sum_{k=1}^{L_t}\beta_t^{ik}(\theta^i)\nu_t^{ik}(\theta^i)\nu_t^{ik}(\theta^i)^T\right)W_t^i(\theta^i)^T - W_t^i(\theta^i)\left(\sum_{k=1}^{L_t}\beta_t^{ik}(\theta^i)\nu_t^{ik}(\theta^i)\right) \cdot \left(\sum_{k'=1}^{L_t}\beta_t^{ik'}(\theta^i)\nu_t^{ik'}(\theta^i)\right)^T W_t^i(\theta^i)^T \tag{31c}$$

with:

$$W_t^i(\theta^i) = \bar{P}_t^i(\theta^i) h^i(\theta^i)^T [\bar{Q}_t^i(\theta^i)]^{-1} \tag{31d}$$

$$\beta_t^{ik}(\theta^i) \triangleq \text{Prob}\{[\Phi(\phi_t)^T]_{i*}[\tilde{\chi}_t]_{*k} = 1 \mid \theta_t^i = \theta^i, Y_t\}$$

$$= \sum_{\substack{\phi,\tilde{\chi},\eta \\ \phi\neq 0 \\ \eta^i=\theta^i}} [\Phi(\phi)^T]_{i*}\tilde{\chi}_{*k}\beta_t(\phi,\tilde{\chi},\eta)/p_{\theta_t^i|Y_t}(\theta^i). \tag{31e}$$

PROOF See Appendix B.

Equation (30a) replaces six nested equations of [18, eqs. (18) and (20)–(24)]. As a direct consequence, Theorem 2 leads to a more compact version of IMMJPDA, the detailed steps of which we give in the next section.

8. TRACK-COALESCENCE-AVOIDING IMMJPDA FILTER

Fitzgerald [24] has shown that less likely permutation hypotheses pruning provides an effective strategy towards reducing JPDA's sensitivity to track coalescence if $\lambda = 0$ and $P_{\text{d}}^i = 1$. In [8] we have shown that for $\lambda > 0$ or $P_{\text{d}}^i < 1$, the appropriate strategy is to prune per (ϕ_t,ψ_t)-hypothesis all but the most likely χ_t-hypothesis prior to measurement updating. This hypothesis pruning strategy is now extended as follows: evaluate all (ϕ_t,ψ_t,θ_t) hypotheses and prune per (ϕ_t,ψ_t,θ_t)-hypothesis all but the most-likely χ_t-hypothesis. For every ϕ, ψ and θ, satisfying $D(\psi) = D(\phi) \le \min\{M, L_t\}$, the most likely χ hypothesis satisfies the mapping $\hat{\chi}_t(\phi,\psi,\theta)$:

$$\hat{\chi}_t(\phi,\psi,\theta) \triangleq \arg\max_{\chi} \beta_t(\phi, \chi^T\Phi(\psi), \theta)$$

where the maximization is over all permutation matrices χ of size $D(\phi)\times D(\phi)$.

The pruning strategy of evaluating all (ϕ,ψ,θ)-hypotheses and only one χ-hypothesis per (ϕ,ψ,θ)-hypothesis implies that we adopt the following pruned hypothesis weights $\hat{\beta}_t(\phi,\psi,\theta)$:

$$\hat{\beta}_t(\phi,\psi,\theta) = \beta_t(\phi, \hat{\chi}(\phi,\psi,\theta)^T\Phi(\psi),\theta)/\hat{c}_t \quad \text{if} \quad 0 < D(\phi) \le \min\{M, L_t\}$$

$$= \beta_t(\{0\}^M, \{\}^{L_t}, \theta)/\hat{c}_t \qquad \text{if} \quad D(\phi) = 0$$

$$= 0 \qquad \text{else}$$

with $\hat{c}_t$ a normalization constant for $\hat{\beta}_t$; i.e. such that

$$\sum_{\substack{\phi,\psi,\theta \\ D(\psi)=D(\phi)}} \hat{\beta}_t(\phi,\psi,\theta) = 1.$$

Through combining the equations of Theorem 2 with the above step, we arrive at the track-coalescence-avoiding IMMJPDA, for short IMMJPDA*:

IMMJPDA* Step 1: For each target this comes down to the interaction step of the IMM algorithm [7] for all $i\in[1,M]$: Starting with

$$\hat{\gamma}_{t-1}^i(\theta^i) \triangleq p_{\theta_{t-1}^i|Y_{t-1}}(\theta^i), \qquad \theta^i \in \mathbb{M}$$

$$\hat{x}_{t-1}^i(\theta^i) \triangleq E\{x_{t-1}^i \mid \theta_{t-1}^i = \theta^i, Y_{t-1}\}, \qquad \theta^i \in \mathbb{M}$$

$$\hat{P}_{t-1}^i(\theta^i) \triangleq E\{[x_{t-1}^i - \hat{x}_{t-1}^i(\theta^i)] \cdot [x_{t-1}^i - \hat{x}_{t-1}^i(\theta^i)]^T \mid \theta_{t-1}^i = \theta^i, Y_{t-1}\}, \qquad \theta^i \in \mathbb{M}$$

one evaluates the mixed initial condition for the filter matched to $\theta_t^i = \theta^i$ as follows (due to (4)):

$$\bar{\gamma}_t^i(\theta^i) = \sum_{\eta^i=1}^{N} \Pi_{\eta^i,\theta^i}^i \cdot \hat{\gamma}_{t-1}^i(\eta^i)$$

$$\hat{x}_{t-1|\theta_t^i}^i(\theta^i) = \sum_{\eta^i=1}^{N} \Pi_{\eta^i,\theta^i}^i \cdot \hat{\gamma}_{t-1}^i(\eta^i)\cdot \hat{x}_{t-1}^i(\eta^i)/\bar{\gamma}_t^i(\theta^i)$$

$$\hat{P}_{t-1|\theta_t^i}^i(\theta^i) = \sum_{\eta^i=1}^{N} \Pi_{\eta^i,\theta^i}^i \cdot \hat{\gamma}_{t-1}^i(\eta^i) \cdot [\hat{P}_{t-1}^i(\eta^i) + [\hat{x}_{t-1}^i(\eta^i) - \hat{x}_{t-1|\theta_t^i}^i(\theta^i)] \cdot [\hat{x}_{t-1}^i(\eta^i) - \hat{x}_{t-1|\theta_t^i}^i(\theta^i)]^T]/\bar{\gamma}_t^i(\theta^i).$$

IMMJPDA* Step 2: Prediction for all $i\in[1,M]$, $\theta^i\in\mathbb{M}$:

$$\bar{x}_t^i(\theta^i) = a^i(\theta^i)\hat{x}_{t-1|\theta_t^i}^i(\theta^i) \tag{32a}$$

$$\bar{P}_t^i(\theta^i) = a^i(\theta^i)\hat{P}_{t-1|\theta_t^i}^i(\theta^i)a^i(\theta^i)^T + b^i(\theta^i)b^i(\theta^i)^T \tag{32b}$$

$$\bar{Q}_t^i(\theta^i) = h^i(\theta^i)\bar{P}_t^i(\theta^i)h^i(\theta^i)^T + g^i(\theta^i)g^i(\theta^i)^T. \tag{32c}$$

IMMJPDA* Step 3: Gating, which is based on [5].

Identify for each target the mode for which Det $\bar{Q}_t^i(\theta)$ is largest:

$$\theta_t^{*i} = \arg\max_{\theta}\{\text{Det}\bar{Q}_t^i(\theta)\}$$

and use this to define for each target i a gate $G_t^i \in \mathbb{R}^m$ as follows:

$$G_t^i \triangleq \{z^i \in IR^m; [z^i - h^i(\theta_t^{*i})\bar{x}_t^i(\theta_t^{*i})]^T \cdot \bar{Q}_t^i(\theta_t^{*i})^{-1}[z^i - h^i(\theta_t^{*i})\bar{x}_t^i(\theta_t^{*i})] \le \kappa\}$$

with κ the gate size. Now we define L_t to denote the number of measurements y_t that are in one or more of the gates G_t^i.

IMMJPDA Step 4:* Evaluation of the detection/association/mode hypotheses is based on Theorem 2; for all $\phi \in \{0,1\}^M$, $\tilde{\chi} \in \{0,1\}^{D(\phi)\times L_t}$, $\theta \in \mathbb{M}^M$,

$$\beta_t(\phi,\tilde{\chi},\theta) \cong \left[\prod_{i=1}^{L_t-D(\phi)} \lambda([\Phi(1_{L_t} - \tilde{\chi}^T\tilde{\chi}1_{L_t})\mathrm{y}_t]_i)\right]$$

$$\cdot \prod_{i=1}^{M}[f_t^i(\phi,\tilde{\chi},\theta^i)\cdot \bar{\gamma}_t^i(\theta^i)$$

$$\cdot (1-P_\mathrm{d}^i\chi_m^2(\kappa))^{(1-\phi_i)}(P_\mathrm{d}^i\chi_m^2(\kappa))^{\phi_i}]/c_t$$

$$\text{if} \quad \tilde{\chi}1_{L_t} = 1_{D(\phi)}$$

$$= 0 \qquad \text{else} \tag{33a}$$

with for $\phi^i = 0$: $f_t^i(\phi,\tilde{\chi},\theta^i) = 1$, and for $\phi^i = 1$:

$$f_t^i(\phi,\tilde{\chi},\theta^i)$$

$$\cong [(2\pi)^m \mathrm{Det}\{\bar{Q}_t^i(\theta^i)\}]^{-\phi_i/2}$$

$$\cdot \exp\left\{-\frac{1}{2}\sum_{k=1}^{L_t}[\Phi(\phi)^T]_{i*}\tilde{\chi}_{*k}\nu_t^{ik}(\theta^i)^T[\bar{Q}_t^i(\theta^i)]^{-1}\nu_t^{ik}(\theta^i)]\right\} \tag{33b}$$

$$\nu_t^{ik}(\theta^i) = \mathrm{y}_t^k - h^i(\theta^i)\bar{x}_t^i(\theta^i). \tag{33c}$$

IMMJPDA Step 5:* Track-coalescence hypothesis pruning.

First, evaluate for every (ϕ,ψ,θ) such that $0 < D(\psi) = D(\phi) \le \min\{M,L_t\}$:

$$\hat{\chi}_t(\phi,\psi,\theta) \triangleq \arg\max_{\chi} \beta_t(\phi,\chi^T\Phi(\psi),\theta).$$

Next, evaluate all $\hat{\chi}_t(\phi,\psi,\theta)$ hypothesis weights:

$$\hat{\beta}_t(\phi,\psi,\theta) = \beta_t(\phi,\hat{\chi}_t(\phi,\psi,\theta)^T\Phi(\psi),\theta)/\hat{c}_t$$

$$\text{if} \quad 0 < D(\psi) = D(\phi) \le \min\{M,L_t\}$$

$$= \beta_t(\{0\}^M,\{\}^{L_t},\theta)/\hat{c}_t$$

$$\text{if} \quad D(\psi) = D(\phi) = 0$$

$$= 0 \qquad \text{else}$$

where $\hat{c}_t$ is a normalizing constant for $\hat{\beta}_t$.

IMMJPDA Step 6:* Measurement update equations (also based on Theorem 2); for all $i \in [1,M]$, $\theta^i \in \mathbb{M}$,

$$\hat{\gamma}_t^i(\theta^i) \cong \sum_{\substack{\phi,\psi,\eta \\ \eta^i=\theta^i}} \hat{\beta}_t(\phi,\psi,\eta) \tag{34a}$$

$$\hat{x}_t^i(\theta^i) \cong \bar{x}_t^i(\theta^i) + W_t^i(\theta^i)\left(\sum_{k=1}^{L_t}\hat{\beta}_t^{ik}(\theta^i)\nu_t^{ik}(\theta^i)\right) \tag{34b}$$

$$\hat{P}_t^i(\theta^i) \cong \bar{P}_t^i(\theta^i) - W_t^i(\theta^i)h^i(\theta^i)\bar{P}_t^i(\theta^i)\left(\sum_{k=1}^{L_t}\hat{\beta}_t^{ik}(\theta^i)\right)$$

$$+ W_t^i(\theta^i)\left(\sum_{k=1}^{L_t}\hat{\beta}_t^{ik}(\theta^i)\nu_t^{ik}(\theta^i)\nu_t^{ik}(\theta^i)^T\right)W_t^i(\theta^i)^T$$

$$- W_t^i(\theta^i)\left(\sum_{k=1}^{L_t}\hat{\beta}_t^{ik}(\theta^i)\nu_t^{ik}(\theta^i)\right)$$

$$\cdot\left(\sum_{k'=1}^{L_t}\hat{\beta}_t^{ik'}(\theta^i)\nu_t^{ik'}(\theta^i)\right)^T W_t^i(\theta^i)^T \tag{34c}$$

with

$$W_t^i(\theta^i) = \bar{P}_t^i(\theta^i)h^i(\theta^i)^T[\bar{Q}_t^i(\theta^i)]^{-1} \tag{34d}$$

$$\hat{\beta}_t^{ik}(\theta^i) = \left(\sum_{\substack{\phi,\psi,\eta \\ \phi,\psi\neq 0 \\ \eta^i=\theta^i}}[\Phi(\phi)^T]_{i*}[\hat{\chi}_t(\phi,\psi,\eta)^T\Phi(\psi)]_{*k}\right.$$

$$\left.\cdot\hat{\beta}_t(\phi,\psi,\eta)\right)\Big/\hat{\gamma}_t^i(\theta^i) \tag{34e}$$

where $[.]_{*k}$ is the kth column of [.] and $[.]_{i*}$ is the ith row of [.].

IMMJPDA Step 7:* Output equations:

$$\hat{x}_t^i = \sum_{\theta^i=1}^{N}\hat{\gamma}_t^i(\theta^i)\cdot\hat{x}_t^i(\theta^i) \tag{35a}$$

$$\hat{P}_t^i = \sum_{\theta^i=1}^{N}\hat{\gamma}_t^i(\theta^i)(\hat{P}_t^i(\theta^i) + [\hat{x}_t^i(\theta^i)-\hat{x}_t^i]\cdot[\hat{x}_t^i(\theta^i)-\hat{x}_t^i]^T). \tag{35b}$$

REMARK 3 By deleting the track coalescence hypothesis pruning Step 5 from IMMJPDA*, and by replacing $\hat{\beta}(\phi,\psi,\eta)$ by $\beta(\phi,\psi,\eta)$ in Steps 6 and 7, we get the compact IMMJPDA filter. As already announced in Remark 2, the reason to refer to compact IMMJPDA is that (33b) replaces six nested equations in the IMMJPDA of [18, eqs. (18) and (20)–(24)].

9. MONTE CARLO SIMULATIONS

In this section some Monte Carlo simulation results are given for the two novel joint particle filters, for the (compact) IMMJPDA and IMMJPDA* filter algorithms, and for a multi-target tracker using an IMM-PDA for each track. The two particle filters ran on a total of $S = 10^4$ joint particles. The simulations aim at gaining insight into the behavior and performance of the filters regarding track maintenance when two targets move in and out of close approach situations, while giving the filters enough time to converge after a maneuver has taken place. In the example scenarios there are two tracked targets, each modeled with two possible modes. The first mode represents a constant velocity model and the second mode represents a constant acceleration model. It is assumed that both targets are initially tracked well, that for their initial track estimates there is no uncertainty regarding which track belongs to which target. Both objects move towards each other, each with constant initial velocity V_{initial}. At a certain moment in time both objects start decelerating with -50 m/s^2 until they both have zero velocity. The moment at which the deceleration starts is such that when the objects both have zero velocity, the distance between the two objects equals d (see Fig. 1). After spending a significant number of scans with zero velocity, both objects start accelerating with 50 m/s^2 away from each other without crossing until their velocity equals the opposite of their initial velocity. From that moment on the velocity of both objects remains constant again (thus the final relative velocity $V_{\text{rel, final}} = V_{\text{rel, initial}}$). Note that $d < 0$ implies that the objects have crossed each other before they have reached zero velocity. In each simulation the filters start with perfect estimates and run for 40 scans. Examples of the trajectories for $d \geq 0$ and $d < 0$ are depicted in Figs. 1(a) and 1(b) respectively.

For each target, the underlying model of the potential target measurements is given by (1) and (2), i.e.:

$$x^i_{t+1} = a^i(\theta^i_{t+1})x^i_t + b^i(\theta^i_{t+1})w^i_t$$
$$z^i_t = h^i(\theta^i_t)x^i_t + g^i(\theta^i_t)v^i_t$$

with for $i \in \{1,2\}$ and $\theta^i_t \in \{1,2\}$:

$$a^i(1) = \begin{bmatrix} 1 & T_s & 0 \\ 0 & 1 & 0 \\ 0 & 0 & 0 \end{bmatrix}, \qquad a^i(2) = \begin{bmatrix} 1 & T_s & \frac{1}{2}T_s^2 \\ 0 & 1 & T_s \\ 0 & 0 & 1 \end{bmatrix}$$

$$b^i(1) = \sigma^i_a \cdot \begin{bmatrix} 0 \\ 0 \\ 1 \end{bmatrix}, \qquad b^i(2) = \sigma^i_a \cdot \begin{bmatrix} 0 \\ 0 \\ 0 \end{bmatrix}$$

$$h^i = [1\ \ 0\ \ 0], \qquad g^i = \sigma^i_m$$

$$\Pi = \begin{bmatrix} 1 - T_s/\tau_1 & T_s/\tau_1 \\ T_s/\tau_2 & 1 - T_s/\tau_2 \end{bmatrix}$$

where σ^i_a represents the standard deviation of acceleration noise and σ^i_m represents the standard deviation of the measurement error. For simplicity we consider the situation of similar targets only; i.e., $\sigma^i_a = \sigma_a$, $\sigma^i_m = \sigma_m$, $P^i_{\text{d}} = P_{\text{d}}$. With this, the scenario parameters are P_{d}, λ, d, V_{initial}, T_s, σ_m, σ_a, τ_1, τ_2, and the gate size γ. We used fixed parameters $\sigma_m = 30$, $\sigma_a = 50$, $\tau_1 = 50$, $\tau_2 = 5$, and $\gamma = 25$. Table I gives the other scenario parameter values that are being used for the Monte Carlo simulations.

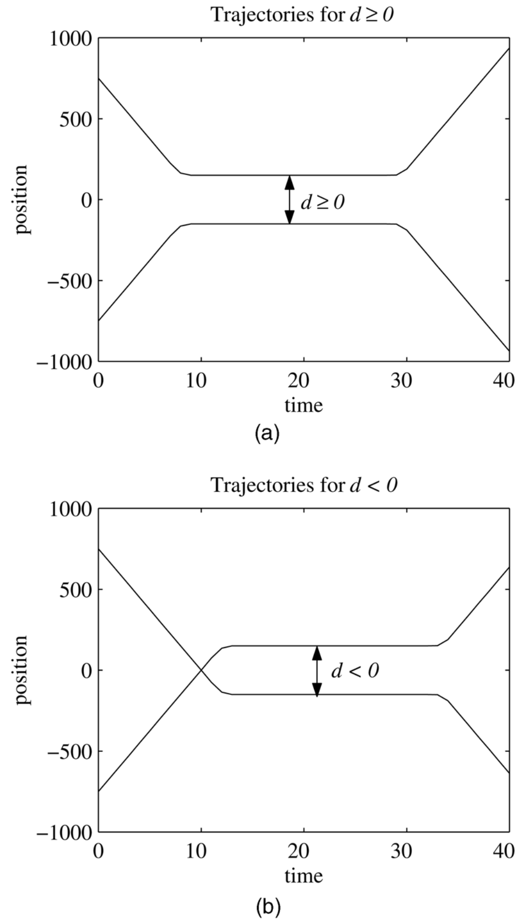

Fig. 1. Trajectories examples for $d \geq 0$ and for $d < 0$.

TABLE I
Scenario Parameter Values[1]

Scenario	P_{d}	λ	d	V_{initial}	T_s
1	1	0	Variable	75	1
2	1	0.001	Variable	75	1
3	0.9	0	Variable	75	1
4	0.9	0.001	Variable	75	1

[1]IMMPDA's $\lambda = 0.00001$ for scenarios 1 and 3.

During our simulations we counted track i "OK" if

$$|h^i\hat{x}^i_T - h^i x^i_T| \leq 9\sigma_m$$

and we counted track $i \neq j$ "Swapped" if

$$|h^i\hat{x}^i_T - h^j x^j_T| \leq 9\sigma_m.$$

Furthermore, two tracks $i \neq j$ are counted "Coalescing" at scan t, if

$$|h^i\hat{x}^i_t - h^j\hat{x}^j_t| \leq \sigma_m \wedge |h^i x^i_t - h^j x^j_t| > \sigma_m.$$

For each of the scenarios Monte Carlo simulations containing 100 runs have been performed for each of the tracking filters. The initial track estimates are

$$\hat{x}_0^1(\theta) = \begin{bmatrix} -750 \\ 75 \\ 0 \end{bmatrix}$$

$$\hat{x}_0^2(\theta) = \begin{bmatrix} 750 \\ -75 \\ 0 \end{bmatrix}, \qquad \theta \in \{1,2\}$$

$$\hat{P}_0^i(1) = \begin{bmatrix} 100 & 0 & 0 \\ 0 & \frac{100}{9} & 0 \\ 0 & 0 & \frac{1}{9} \end{bmatrix}$$

$$\hat{P}_0^i(2) = \begin{bmatrix} 100 & 0 & 0 \\ 0 & \frac{100}{9} & 0 \\ 0 & 0 & \frac{1}{36} \end{bmatrix}$$

$$\hat{\gamma}_0^i(1) = 0.9, \qquad \hat{\gamma}_0^i(2) = 0.1 \qquad \text{for} \quad i = 1,2.$$

The results of the Monte Carlo simulations for the four scenarios are shown in tables and figures as follows:

- The percentage of Both tracks "OK," see Table II, and Figs. 2(a), 3(a), 4(a) and 5(a).
- The percentage of Both tracks "OK" or "Swapped," see Table III, and Figs. 2(b), 3(b), 4(b) and 5(b).
- The average number of "Coalescing" scans, see Table IV, and Figs. 2(c), 3(c), 4(c) and 5(c).
- The average CPU time per scan (in seconds), see Table V.

TABLE II
Average % Both Tracks "OK"

Scen.	IMMPDA	IMMJPDA	IMMJPDA*	SIR Joint	SIR-H Joint
1	19	66	73	70	75
2	10	56	68	65	70
3	6	63	69	70	72
4	4	41	50	43	57

TABLE III
Average % Both Tracks "OK" or "Swapped"

Scen.	IMMPDA	IMMJPDA	IMMJPDA*	SIR Joint	SIR-H Joint
1	28.3	99.96	100	97.8	96.2
2	18.9	92.5	96.8	91.6	94.6
3	8.5	99.8	100	97.6	95.8
4	5.6	76.6	80.96	66.0	82.3

TABLE IV
Average Number of Coalescing Scans

Scen.	IMMPDA	IMMJPDA	IMMJPDA*	SIR Joint	SIR-H Joint
1	9.7	1.5	0.4	1.2	1.3
2	11.0	2.1	0.3	1.2	1.4
3	18.9	1.7	0.5	1.3	1.3
4	14.5	2.6	0.5	1.3	1.5

TABLE V
Average CPU Time Per Scan (in milliseconds)

Scen.	IMMPDA	IMMJPDA	IMMJPDA*	SIR Joint	SIR-H Joint
1	16	22	23	385	439
2	38	54	48	7245	7959
3	14	20	20	377	438
4	38	61	56	7170	7810

The results in Tables II–IV and Figs. 2–5 show that for targets that come close to each other, IMMJPDA, IMMJPDA* and the particle filters perform much better than IMMPDA. As expected, these simulation results show increased difficulty for $P_d = 0.9$ when compared to $P_d = 1$ and for $\lambda = 0.001$ when compared to $\lambda = 0$. Furthermore $\lambda = 0.001$ has more impact on the performance than $P_d = 0.9$. This can be explained by the fact that for $\lambda = 0.001$ a target track may diverge because of false measurements. The SIR-H joint particle filter suffers the least from this.

Measured in terms of "both tracks OK" (Table II and Figs. 2(a)–5(a)) the SIR-H joint particle filter performed best, the IMMJPDA* second best, the SIR-H joint particle filter third and the IMMJPDA fourth. The both tracks "OK" Figs. 2(a)–5(a) show a slight difference for $d < 0$ and $d > 0$. This is because for $d < 0$ the target trajectories cross each other before they have reached zero velocity, while for $d > 0$ they do not cross (see Fig. 1).

Figs. 2(a)–5(a) show that IMMJPDA and IMMJPDA* filters have oscillating variation in performance which is lacking for SIR-H joint particle filter. This phenomenon can be explained by the observation that the effect of "overshoot" during a maneuver is for IMMJPDA and IMMJPDA* more profound than for the SIR-H joint particle filter, because the latter filters perform time extrapolation from only one state estimate per mode, whereas the SIR-H joint particle filter performs time extrapolation for many particles per mode. The effect is that for some d values IMMJPDA and IMMJPDA* actually benefit from overshoot in the sense that it keeps the tracks separated, while for other d values the overshoot actually moves the tracks closer to each other. This effect is less profound for the SIR-H joint particle filters due to time extrapolation for many particles per mode; hence oscillating variation in performance does not occur.

Rather surprisingly, IMMJPDA* outperforms Hybrid SIR joint particle filter regarding the both tracks "OK" or "Swapped" criterion (Table III and Figs. 2(b)–5(b)) on the "easy" scenarios 1–3. Scenario 4 shows that IMMJPDA* is outperformed on this criterion by the SIR-H joint particle filter when missing and false measurement conditions become more challenging.

Table IV and Figs. 2(c)–5(c) show that IMMJPDA* performs best on track coalescence avoidance. Next best

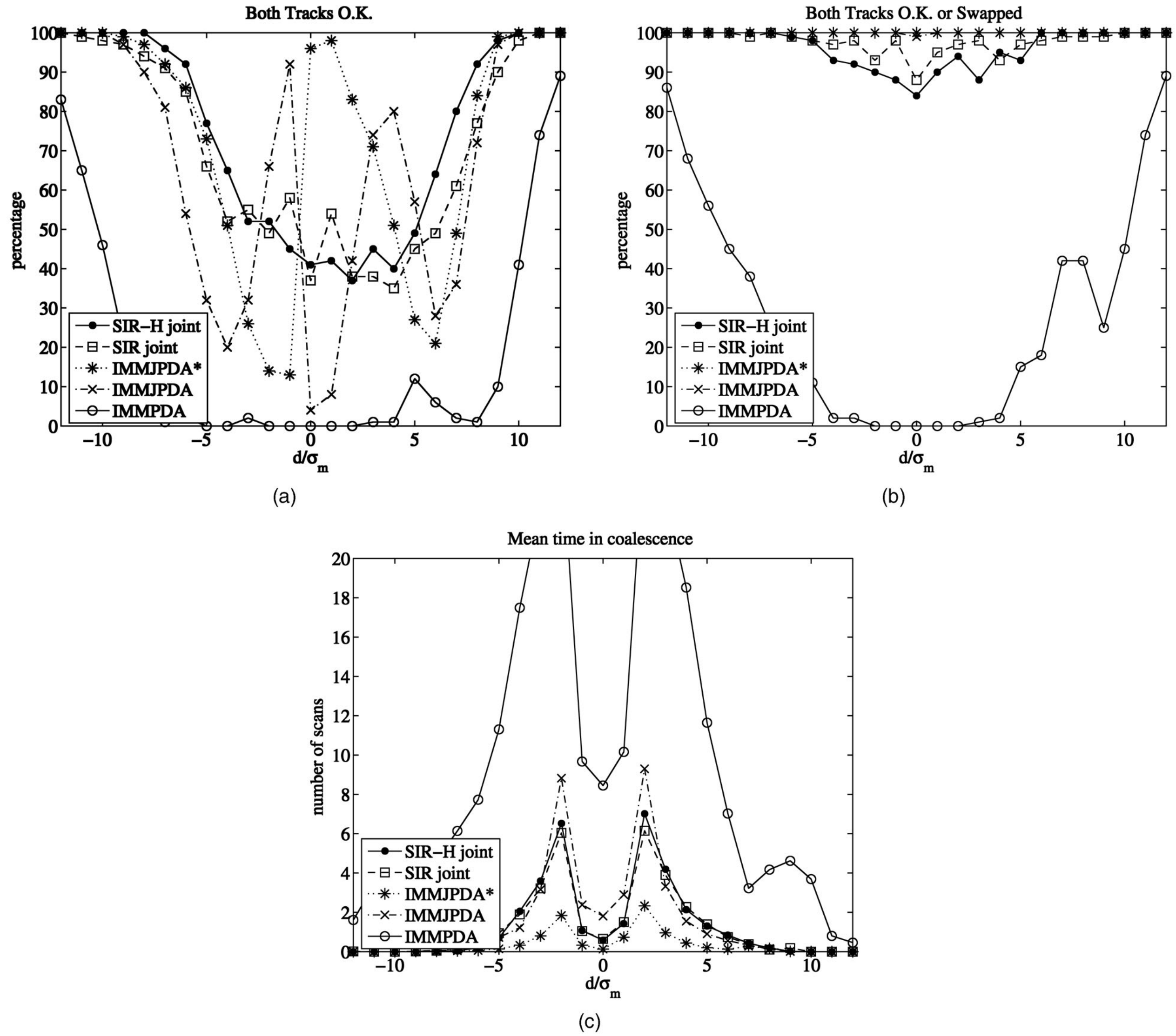

Fig. 2. Simulation results for scenario 1. (a) Both tracks "OK" percentage. (b) Both tracks "OK" or "Swapped" percentage. (c) Average number of "Coalescing" scans.

are the two particle filters, and fourth is IMMJPDA. The "dip" in "mean time in coalescence" around zero is due to the definition of "coalescing tracks." That is, when the targets are actually moving very close to each other, which is the case for small d values, there are no coalescing scans counted. Scans are only counted coalescing when the targets are separated from each other far enough.

Table V indicates a significant CPU-time increase for joint particle filters relative to the others. The increase is one order of magnitude for scenarios without clutter and two orders of magnitude for scenarios with clutter.

It should be noticed that there are various complementary methods available that allow to reduce the number of particles and/or CPU time significantly without reducing performance (e.g. [1], [38]). Hence when reading Table V one should be aware that these methods have not been investigated in this paper.

10. CONCLUDING REMARKS

In this paper we studied the problem of maneuvering target tracking from possibly missing and false measurements. The density of the false measurements was assumed to be non-homogeneous. For this problem we studied particle filtering as an alternative to multi-target track maintenance versions of IMM in combination with PDA or JPDA. The approach taken is to first characterize the problem in terms of filtering for a jump linear descriptor system with both Markovian and i.i.d. coefficients, and next to use this for the derivation of the exact recursive equation for the Bayesian filter (Theorem 1). This result has been used to develop two SIR type particle filters, one which resamples a fixed number of joint particles (SIR joint particle filter) and one which resamples a fixed number of joint particles per joint mode (SIR-H joint particle filter). We have also shown that application of the approximating assumptions of [18] to

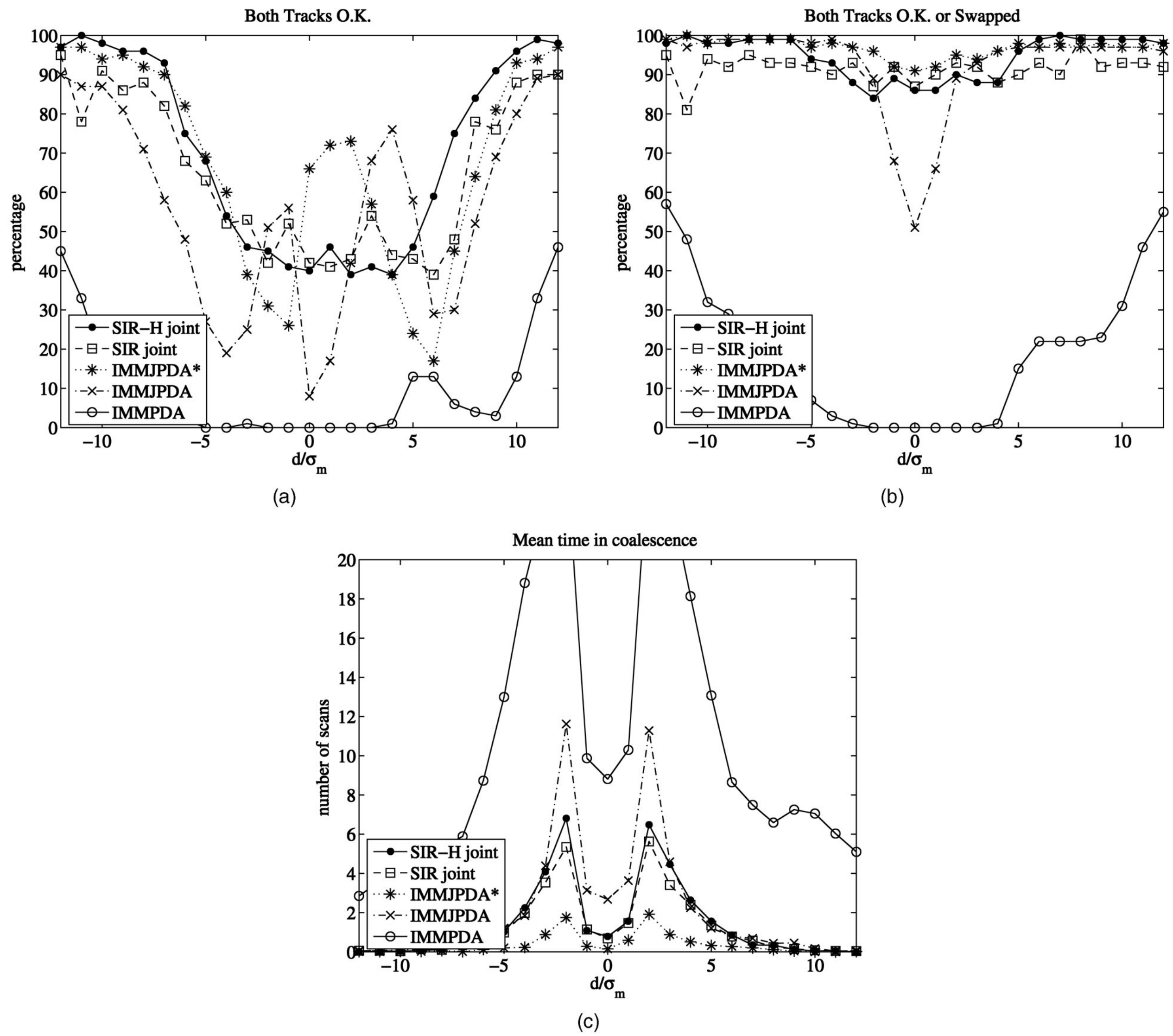

Fig. 3. Simulation results for scenario 2. (a) Both tracks "OK" percentage. (b) Both tracks "OK" or "Swapped" percentage. (c) Average number of "Coalescing" scans.

the exact Bayesian filter equations (Theorem 2) leads to a compact version of their IMMJPDA filter equations. For this (compact) IMMJPDA filter we also developed a track-coalescence-avoiding version (IMMJPDA*) by introduction of a particular pruning of permutation hypotheses. All our four novel filter algorithms cover the situation of non-homogeneous density of false measurements.

Through Monte Carlo simulations for a series of simple scenarios with two targets and two associated tracks these four novel filters have been compared to each other and to a filter which runs a single target IMMPDA (per track). All four clearly outperformed IMMPDA. The particle filters used 10^4 joint particles; with this the SIR-H joint particle filter appears to approximate the Bayesian filter well, whereas the SIR joint particle filter did not. On all scenarios, IMMJPDA* performs significantly better than IMMJPDA and sometimes even remarkably close to the performance of the SIR-H joint particle filter. Apparently, the performance reduction by the IMMJPDA approximation of the exact Bayesian filter can be partly compensated by introducing the additional IMMJPDA* approximation. IMMJPDA and IMMJPDA* both perform less well than the SIR-H joint PF on the following two points:

- The performance of both IMMJPDA and IMMJPDA* varies heavily with changes in the geometry of encountering target paths; this varying kind of behavior is not shown by the SIR-H joint particle filter;
- The SIR-H joint particle filter is least sensitive to divergence of track because of switching to running on false measurements; this advantage shows both when targets are clearly separated from each other and when target paths come close to each other.

Recently both [12] and [47] explored the potential effect on performance of extending IMMJPDA and

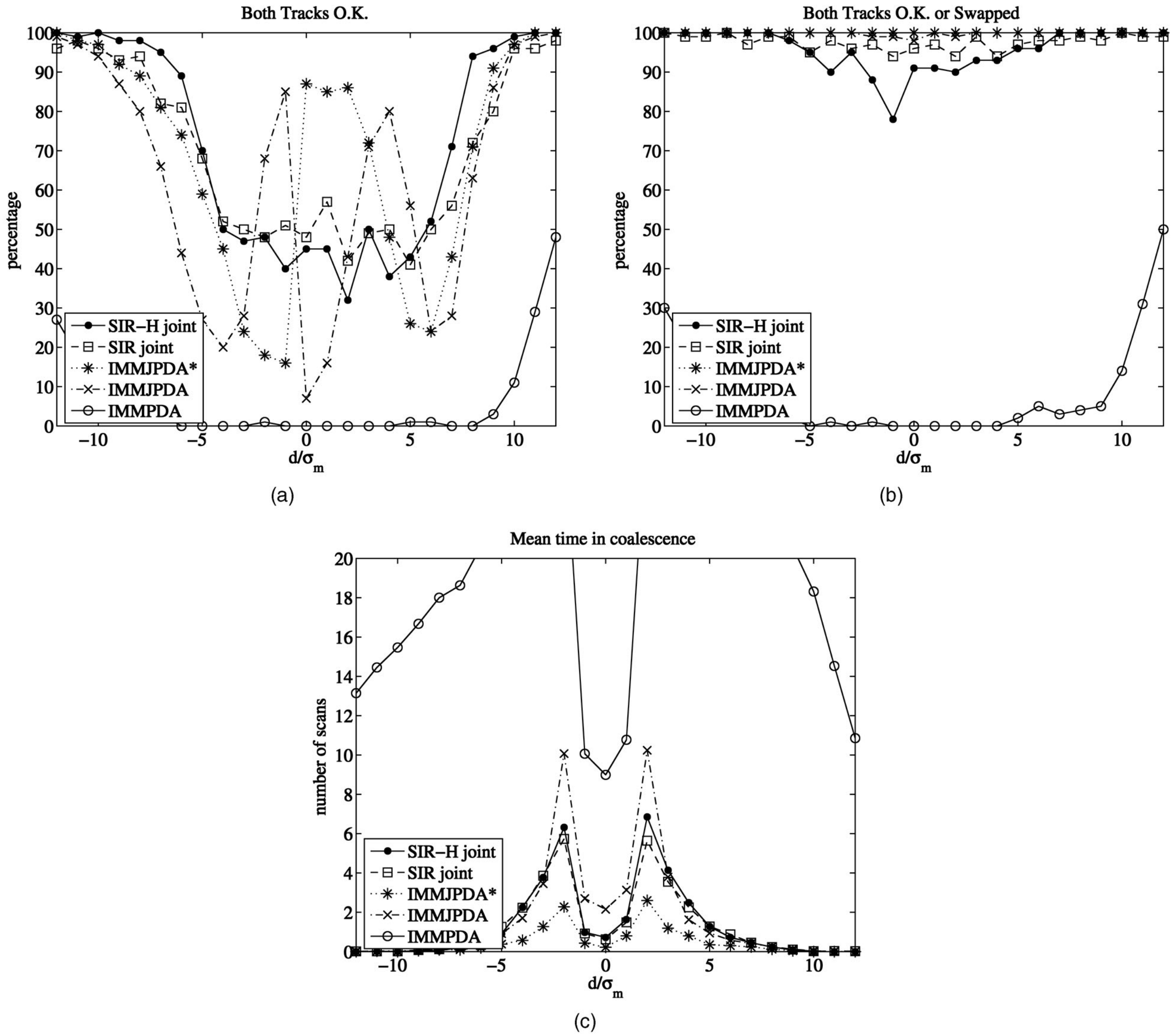

Fig. 4. Simulation results for scenario 3. (a) Both tracks "OK" percentage. (b) Both tracks "OK" or "Swapped" percentage. (c) Average number of "Coalescing" scans.

IMMJPDA* to joint tracking versions, i.e., to versions where the multi-target states/modes are jointly estimated. Tugnait [47] showed slightly improved simulation results for a particular example. In [12] we showed examples where the joint tracking versions performed better and examples where they performed worse. On average, the joint tracking versions even performed worse. In [14], [13] we showed that an appropriate pruning of permutation hypothesis also yields a track-coalescence-avoiding joint tracking version. The two weak points listed above for IMMJPDA and IMMJPDA* also apply to these joint versions.

Because the computational load of IMMJPDA* is one to two orders of magnitude lower than the computational load of the SIR-H joint particle filter is, this may be a fair reason to prefer IMMJPDA* over the SIR-H joint particle filter for particular applications. One should also be aware that the efficiency of the SIR-H joint particle filter can be significantly improved by incorporating various methods from literature (e.g. [1, 38, 42]).

In addition to the option of improving the efficiency of the SIR-H joint particle filtering, it is an option to improve the adaptation of the output equations. In this paper we considered the mean and covariance of target states only, and thus averaged over the states of all particles. One alternative approach might be trying to incorporate the permutation hypothesis pruning strategy of IMMJPDA* within the output equations of the SIR-H joint particle filter. Another direction [32] is to apply clustering of particles prior to averaging.

There are several other interesting extensions possible for the jump-linear descriptor framework and the novel exact and approximate filters. For example, to incorporate the target initiation and termination approach of [39], or to incorporate unresolved measurements (e.g. [31]).

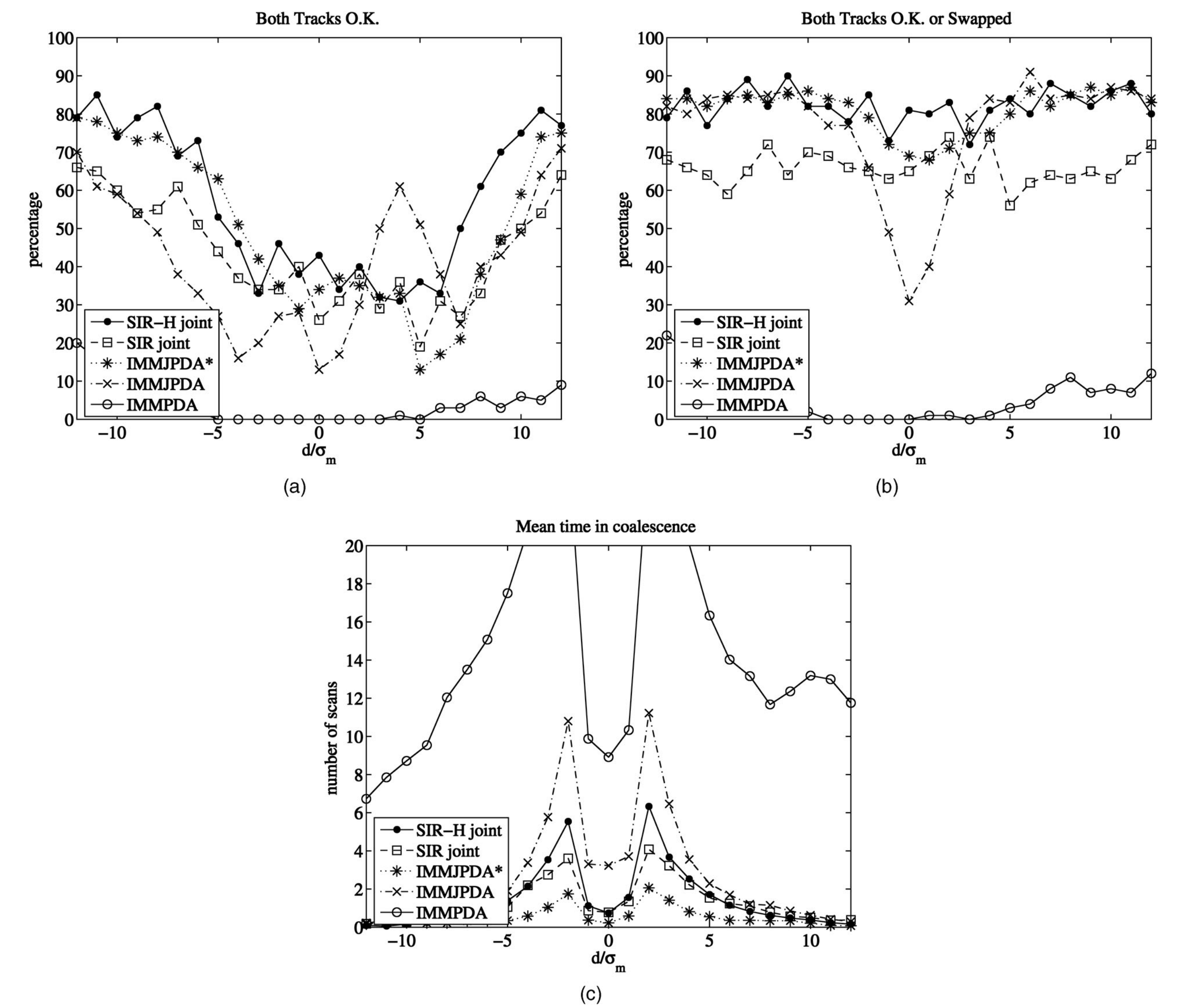

Fig. 5. Simulation results for scenario 4. (a) Both tracks "OK" percentage. (b) Both tracks "OK" or "Swapped" percentage. (c) Average number of "Coalescing" scans.

Appendix A

PROOF If $\phi = 0$ we get

$$p_{x_t|\theta_t,\phi_t,\tilde{\chi}_t,Y_t}(x \mid \theta, 0, \tilde{\chi}) = p_{x_t|\theta_t,Y_{t-1}}(x \mid \theta). \tag{A1}$$

Else, i.e., $\phi \neq 0$:

$$\begin{aligned} p_{x_t|\theta_t,\phi_t,\tilde{\chi}_t,Y_t}&(x \mid \theta, \phi, \tilde{\chi}) \\ &= p_{x_t|\theta_t,\phi_t,\tilde{\chi}_t,\mathrm{y}_t,L_t,Y_{t-1}}(x \mid \theta,\phi,\tilde{\chi},\mathrm{y}_t,L_t) \\ &= p_{x_t|\theta_t,\phi_t,\tilde{\chi}_t,\mathrm{y}_t,L_t,\tilde{\mathrm{y}}_t,Y_{t-1}}(x \mid \theta,\phi,\tilde{\chi},\mathrm{y}_t,L_t,\tilde{\boldsymbol{\chi}}\mathrm{y}_t) \\ &= p_{x_t|\theta_t,\phi_t,\tilde{\mathrm{y}}_t,Y_{t-1}}(x \mid \theta,\phi,\tilde{\boldsymbol{\chi}}\mathrm{y}_t) \\ &= p_{\tilde{z}_t|x_t,\theta_t,\phi_t}(\tilde{\boldsymbol{\chi}}\mathrm{y}_t \mid x,\theta,\phi) \cdot p_{x_t|\theta_t,Y_{t-1}}(x \mid \theta)/F_t(\phi,\tilde{\chi},\theta) \end{aligned} \tag{A2}$$

with

$$F_t(\phi,\tilde{\chi},\theta) \stackrel{\Delta}{=} p_{\tilde{z}_t|\theta_t,\phi_t,Y_{t-1}}(\tilde{\boldsymbol{\chi}}\mathrm{y}_t \mid \theta,\phi). \tag{A3}$$

Subsequently

$$\begin{aligned} \beta_t(\phi,\tilde{\chi},\theta) &\stackrel{\Delta}{=} \mathrm{Prob}\{\phi_t = \phi, \tilde{\chi}_t = \tilde{\chi}, \theta_t = \theta \mid Y_t\} \\ &= p_{\phi_t,\tilde{\chi}_t,\theta_t|Y_t}(\phi,\tilde{\chi},\theta) \\ &= p_{\phi_t,\tilde{\chi}_t\theta_t|\mathrm{y}_t,L_t,Y_{t-1}}(\phi,\tilde{\chi},\theta \mid \mathrm{y}_t, L_t) \\ &= p_{\mathrm{y}_t,\tilde{\chi}_t,\theta_t|\phi_t,L_t,Y_{t-1}}(\mathrm{y}_t,\tilde{\chi},\theta \mid \phi, L_t) \\ &\quad \cdot p_{\phi_t|L_t,Y_{t-1}}(\phi \mid L_t)/c_t' \\ &= p_{\mathrm{y}_t,\tilde{\chi}_t|\theta_t,\phi_t,L_t,Y_{t-1}}(\mathrm{y}_t,\tilde{\chi} \mid \theta,\phi,L_t) \\ &\quad \cdot p_{\phi_t|L_t,Y_{t-1}}(\phi \mid L_t) p_{\theta_t|Y_{t-1}}(\theta)/c_t'. \end{aligned} \tag{A4}$$

If $\phi \neq 0$, we have $D_t > 0$ and

$$\tilde{\chi}_t^T \tilde{\chi}_t = \Phi(\psi_t)^T \chi_t \chi_t^T \Phi(\psi_t) = \Phi(\psi_t)^T \Phi(\psi_t) = \mathrm{Diag}\{\psi_t\}. \tag{A5}$$

Hence

$$\psi_t = \mathrm{Diag}\{\psi_t\} 1_{L_t} = \tilde{\chi}_t^T \tilde{\chi} 1_{L_t}$$

with 1_{L_t} an L_t column vector with L_t 1-valued components.

Moreover, because

$$\tilde{\chi}_t \Phi(\psi_t)^T = \chi_t^T \Phi(\psi_t)\Phi(\psi_t)^T = \chi_t^T \tag{A6}$$

this shows that the transformation from (ψ_t, χ_t) into $\tilde{\chi}_t$ has an inverse. For the first term on the right hand side of (A.4) this implies:

$$p_{y_t,\tilde{\chi}_t|\theta_t,\phi_t,L_t,Y_{t-1}}(y_t, \chi^T\Phi(\psi) \mid \theta, \phi, L_t) = p_{y_t,\psi_t,\chi_t|\theta_t,\phi_t,L_t,Y_{t-1}}(y_t, \psi, \chi \mid \theta, \phi, L_t). \tag{A7}$$

Furthermore, because the transformation from (y_t, ψ_t, χ_t) into $(\tilde{z}_t, f_t, \psi_t, \chi_t)$ is a permutation, we get for $L_t > D(\phi) > 0$

$$p_{y_t,\psi_t,\chi_t|\theta_t,\phi_t,L_t,Y_{t-1}}(y_t, \psi, \chi \mid \theta, \phi, L_t) = p_{\tilde{z}_t,f_t,\psi_t,\chi_t|\theta_t,\phi_t,L_t,Y_{t-1}}(\boldsymbol{\chi}^T\boldsymbol{\Phi}(\psi)y_t, \boldsymbol{\Phi}(1_{L_t} - \psi)y_t, \psi, \chi \mid \theta, \phi, L_t). \tag{A8}$$

Substituting (A8) in (A7) and this into (A4) yields:

$$\beta_t(\phi, \chi^T\Phi(\psi), \theta) = p_{\tilde{z}_t,f_t,\psi_t,\chi_t|\theta_t,\phi_t,L_t,Y_{t-1}}(\boldsymbol{\chi}^T\boldsymbol{\Phi}(\psi)y_t, \boldsymbol{\Phi}(1_{L_t} - \psi)y_t, \psi, \chi \mid \theta, \phi, L_t) \cdot p_{\phi_t|L_t,Y_{t-1}}(\phi \mid L_t) p_{\theta_t|Y_{t-1}}(\theta)/c_t'. \tag{A9}$$

Hence, for $L_t > D(\phi) > 0$, this yields:

$$\beta_t(\phi, \chi^T\Phi(\psi), \theta) = p_{\tilde{z}_t|\theta_t,\phi_t,Y_{t-1}}(\boldsymbol{\chi}^T\boldsymbol{\Phi}(\psi)y_t \mid \theta, \phi) \cdot p_{f_t|\phi_t,\psi_t,L_t}(\boldsymbol{\Phi}(1_{L_t} - \psi)y_t \mid \phi, \psi) p_{\psi_t|\phi_t,L_t}(\psi \mid \phi) \cdot p_{\chi_t|\phi_t}(\chi \mid \phi) p_{L_t|\phi_t}(L_t \mid \phi) p_{\phi_t}(\phi) p_{\theta_t|Y_{t-1}}(\theta)/c''. \tag{A10}$$

Evaluation of the terms in (A10) yields:

$$p_{f_t|\phi_t,\psi_t,L_t}(\boldsymbol{\Phi}(1_{L_t} - \psi)y_t \mid \phi, \psi) = p_{f_t|F_t,\psi_t}(\boldsymbol{\Phi}(1_{L_t} - \psi)y_t \mid L_t - D(\phi), \psi) \overset{(6b)}{=} \prod_{i=1}^{L_t - D(\phi)} p_f([\Phi(1_{L_t} - \psi)y_t]_i) = \prod_{i=1}^{L_t - D(\phi)} p_f([\Phi(1_{L_t} - \tilde{\chi}^T\tilde{\chi}1_{L_t})y_t]_i) \tag{A11}$$

$$p_{\psi_t|\phi_t,L_t}(\psi \mid \phi, L_t) = D(\phi)!(L_t - D(\phi))!/L_t! \tag{A12}$$

$$p_{\chi_t|\phi_t}(\chi \mid \phi) = 1/D(\phi)! \tag{A13}$$

$$p_{L_t|\phi_t}(L_t \mid \phi) = p_{F_t}(L_t - D(\phi)) = (\hat{F}_t)^{(L_t - D(\phi))}\exp\{-\hat{F}_t\}/(L_t - D(\phi))! \quad \text{if} \quad L_t \geq D(\phi); \quad = 0 \quad \text{if} \quad L_t < D(\phi) \tag{A14}$$

$$p_{\phi_t}(\phi) = \prod_{i=1}^{M}[(P_\mathrm{d}^i)^{\phi_i}(1 - P_\mathrm{d}^i)^{1-\phi_i}]. \tag{A15}$$

Substituting (A3) and (A11) through (A15) into (A10) and subsequent evaluation yields for $L_t > D(\phi) > 0$:

$$\beta_t(\phi, \chi^T\Phi(\psi), \theta) = F_t(\phi, \chi^T\Phi(\psi), \theta) \cdot \hat{F}_t^{(L_t - D(\phi))} \cdot \prod_{j=1}^{L_t - D(\phi)} p_f([\Phi(1_{L_t} - \tilde{\chi}^T\tilde{\chi}1_{L_t})y_t]_j) \cdot \prod_{i=1}^{M}[(P_d^i)^{\phi_i}(1 - P_d^i)^{(1-\phi_i)}] \cdot p_{\theta_t|Y_{t-1}}(\theta)/c_t$$

with c_t a normalizing constant. It can be easily verified that the last equation also holds true if $L_t = D(\phi)$ or if $D(\phi) = 0$. Together with (6c) this yields (14).

Appendix B

PROOF From the proof of Proposition 1 we have

$$F_t(\phi, \tilde{\chi}, \theta) = p_{\tilde{z}_t|\theta_t,\phi_t}(\tilde{\boldsymbol{\chi}}y_t \mid \theta, \phi) = \int_{\mathbb{R}^{Mn}} p_{\tilde{z}_t|x_t,\theta_t,\phi_t,Y_{t-1}}(\tilde{\boldsymbol{\chi}}y_t \mid x, \theta, \phi) \cdot p_{x_t|\theta_t,\phi_t,Y_{t-1}}(x, \theta)dx \tag{B1}$$

$$p_{\tilde{z}_t|x_t,\theta_t,\phi_t}(\tilde{\boldsymbol{\chi}}y_t \mid x, \theta, \phi) = \prod_{\substack{i=1 \\ \phi^i=1}}^{M} p_{\tilde{z}_t^i|x_t^i,\theta_t^i}([\Phi(\phi)\tilde{\chi}]_{ik}y_t^k \mid x^i, \theta^i). \tag{B2}$$

This together with C2) yields:

$$F_t(\phi, \tilde{\chi}, \theta) = \prod_{i=1}^{M} f_t^i(\phi, \tilde{\chi}, \theta) \tag{B3}$$

with

$$f_t^i(\phi, \tilde{\chi}, \theta) = \int_{\mathbb{R}^n} p_{\tilde{z}_t^i|x_t^i,\theta_t^i}([\Phi(\phi)\tilde{\chi}]_{ik}y_t^k \mid x^i, \theta^i) \cdot p_{x_t^i|\theta_t^i,Y_{t-1}}(x^i \mid \theta^i)dx^i \quad \text{if} \quad \phi^i = 1; \quad = 1 \quad \text{if } \phi^i = 0. \tag{B4}$$

Together with C3) the last two equations yield (29) and (30a,b,c).

Substitution of (B2) and C2) into (13) yields

$$p_{x_t^i|\theta_t^i,\phi_t,\tilde{\chi}_t,Y_t}(x^i \mid \theta^i, \phi, \tilde{\chi}) = \frac{p_{z_t^i|x_t^i,\theta_t^i}([\Phi(\phi)\tilde{\chi}]_{ik}y_t^k \mid x^i, \theta^i) \cdot p_{x_t^i|\theta_t^i,Y_{t-1}}(x^i \mid \theta^i)}{f_t^i(\phi, \tilde{\chi}, \theta)}. \tag{B5}$$

If $p_{x_t^i|\theta_t^i,Y_{t-1}}(x^i \mid \theta^i)$ is Gaussian with mean $\bar{x}_t^i(\theta^i)$ and covariance $\bar{P}_t^i(\theta^i)$, then the density $p_{x_t^i|\phi_t,\tilde{\chi}_t,\theta_t^i,Y_t}(x^i \mid \phi, \tilde{\chi}, \theta^i)$ is Gaussian with mean $\hat{x}_t^i(\phi, \tilde{\chi}, \theta^i)$ and covariance $\hat{P}_t^i(\phi, \theta^i)$ satisfying for $\phi^i \neq 0$,

$$\hat{x}_t^i(\phi, \tilde{\chi}, \theta^i) = \bar{x}_t^i(\theta^i) + K_t^i(\phi, \theta^i)[[\tilde{\boldsymbol{\chi}}y_t]_i - h^i(\theta^i)\bar{x}_t^i(\theta^i)]$$

$$\hat{P}_t^i(\phi, \theta^i) = \bar{P}_t^i(\theta^i) - K_t^i(\phi, \theta^i)h^i(\theta^i)\bar{P}_t^i(\theta^i)$$

and for $\phi^i = 0$:

$$\hat{x}_t^i(\phi, \tilde{\chi}, \theta^i) = \bar{x}_t^i(\theta^i)$$
$$\hat{P}_t^i(\phi, \theta^i) = \bar{P}_t^i(\theta^i)$$

Hence, $p_{x_t^i|\theta_t^i, Y_t}(. \mid \theta^i)$ is a Gaussian mixture, and all equations in Theorem 2 follow from a lengthy but straightforward evaluation of this mixture.

Acknowledgment

The authors would like to thank the anonymous reviewers for valuable suggestions in improving the paper.

REFERENCES

[1] M. S. Arulampam, S. Maskell, N. Gordon and J. Clapp
A tutorial on particle filters for online nonlinear/non-Gaussian Bayesian trackers.
IEEE Transactions on Signal Procesing, **50** (2002), 174–188.

[2] D. Avitzour
Stochastic simulation Bayesian approach to multitarget tracking.
IEE Proceedings—Radar, Sonar and Navigation, **142** (1995), 41–44.

[3] Y. Bar-Shalom, S. Challa and H. A. P. Blom
IMM estimator versus optimal estimator for hybrid systems.
IEEE Transactions on Aerospace and Electronic Systems, **41** (2005), 986–991.

[4] Y. Bar-Shalom, K. C. Chang and H. A. P. Blom
Tracking splitting targets in clutter using an interacting multiple model joint probabilistic data association filter.
Multitarget Multisensor Tracking, Vol. II, Artech House, 1992, 93–110.

[5] Y. Bar-Shalom and R. Li
Multitarget-multisensor tracking: Principles and techniques. 1995.

[6] H. A. P. Blom
An efficient filter for abruptly changing systems.
In *Proceedings of 23th IEEE Conference on Decision and Control*, 1984, 656–658.

[7] H. A. P. Blom and Y. Bar-Shalom
The interacting multiple model algorithm for systems with Markovian switching coefficients.
IEEE Transactions on Automatic Control, **33** (1988), 780–783.

[8] H. A. P. Blom and E. A. Bloem
Probabilistic data association avoiding track coalescence.
IEEE Transactions on Automatic Control, **45** (2000), 247–259.

[9] H. A. P. Blom and E. A. Bloem
Combining IMM and JPDA for tracking multiple maneuvering targets in clutter.
In *Proceedings of 5th International Conference on Information Fusion*, Annapolis, MD, July 8–11, 2002, Vol. 1, 705–712.

[10] H. A. P. Blom and E. A. Bloem
Interacting multiple model joint probabilistic data association avoiding track coalescence.
In *Proceedings of IEEE Conference on Decision and Control*, Dec, 2002, 3408–3415.

[11] H. A. P. Blom and E. A. Bloem
Joint IMMPDA particle filter.
In *Proceedings of Fusion 2003*, Cairns, Australia, July 2003.

[12] H. A. P. Blom and E. A. Bloem
Tracking multiple maneuvering targets by joint combinations of IMM and PDA.
In *Proceedings of 42nd IEEE Conference on Decision and Control*, Maui, 2003.

[13] H. A. P. Blom and E. A. Bloem
Joint IMM and coupled PDA to track closely spaced targets and to avoid track coalescence.
In *Proceedings of Fusion 2004*, Stockholm, Sweden.

[14] H. A. P. Blom and E. A. Bloem
Exact Bayesian filter and joint IMM coupled PDA tracking of maneuvering targets from possibly missing and false measurements.
Automatica, **42** (2006), 127–135.

[15] Y. Boers and J. N. Driessen
Particle filter based detection for tracking.
In *Proceedings of American Control Conference*, June 2001, 4393–4397.

[16] Y. Boers and H. Driessen
Hybrid state estimation: A target tracking application.
Automatica, **38** (2002), 2153–2158.

[17] Y. Boers, J. N. Driessen, F. Verschure, W. P. M. H. Heemels and A. Juloski
A multi target track before detect application.
In *Proceedings of IEEE Conference on Computer Vision and Pattern Recognition*, June 2003.

[18] B. Chen and J. K. Tugnait
Tracking of multiple maneuvering targets in clutter using IMM/JPDA filtering and fixed-lag smoothing.
Automatica, **37** (2001), 239–249.

[19] L. Dai
Singular control systems.
Lecture notes in Control and Information Sciences, Vol. 118, Springer, 1989.

[20] M. De Feo, A. Graziano, R. Miglioli and A. Farina
IMMJPDA versus MHT and Kalman filter with NN correlation: Performance comparison.
IEE Proceedings—Radar, Sonar and Navigation, **144** (1997), 49–56.

[21] A. Doucet
On sequential simulation-based methods for Bayesian filtering.
Technical Report CUED/F-INFENG/TR.310, Department of Engineering, University of Cambridge, 1998.

[22] A. Doucet, N. J. Gordon and V. Krishnamurthy
Particle filters for state estimation of jump Markov linear systems.
IEEE Transactions on Signal Processing, **49** (2001), 613–624.

[23] R. J. Elliott, F. Dufour and D. D. Sworder
Exact hybrid filters in discrete time.
IEEE Transactions Automatic Control, **41** (1996), 1807–1810.

[24] R. J. Fitzgerald
Development of practical PDA logic for multitarget tracking by micro processor," In Y. Bar-Shalom (Ed.), *Multitarget-Multisensor Tracking*, Artech House, 1990, 1–23.

[25] M. Gauvrit
Bayesian adaptive filter for tracking with measurements of uncertain origin.
Automatica, **20** (1984), 217–224.

[26] N. J. Gordon
A hybrid bootstrap filter for target tracking in clutter.
IEEE Transactions on Aerospace and Electronic Systems, **33** (1997), 353–358.

[27] N. Gordon, D. Salmon and D. Fisher
Bayesian target tracking after group pattern distortion.
In *Proceedings of SPIE*, 1997, 238–248.

[28] N. J. Gordon, D. J. Salmond and A. F. M. Smith
Novel approach to nonlinear/non-Gaussian Bayesian state estimation.
IEE Proceedings, Part F, **140** (1993), 107–113.

[29] C. Hue, J. P. Le Cadre and P. Perez
Tracking multiple objects with particle filtering.
IEEE Transactions on Aerospace and Electronic Systems, **38** (2002), 791–811.

[30] R. Karlsson and F. Gustafsson
Monte Carlo data association for multiple target tracking.
In *Proceedings of IEE Seminar Target Tracking: Algorithms and Applications*, Oct. 2001, 13/1–13/5.

[31] W. Koch and G. Van Keuk
MHT maintenance with possibly unresolved measurements.
IEEE Transactions on Aerospace and Electronic Systems, **33** (1997), 883–892.

[32] C. Kreucher, K. Kastella and A. O. Hero
Tracking multiple targets using a particle filter representation of the joint multitarget probability density.
In *Proceedings of SPIE International Symposium on Optical Science and Technology*, San Diego, CA, Aug. 2003.

[33] J. MacCormick and A. Blake
A probabilistic exclusion principle for tracking multiple objects.
In *Proceedings of 7th International Conference on Computer Vision*, Greece, 1999, 572–580.

[34] J. MacCormick and M. Isard
Bramble: A Bayesian multiple-blob tracker.
In *Procedings of 8th International Conference on Computer Vision*, Vancouver, July 2001, 34–41.

[35] S. Maskell, M. Rollason, N. Gordon and D. Salmond
Efficient particle filtering for multiple target tracking with application to tracking in structured images.
In *Proceedings on Signal and Data Processing of Small Targets*, Orlando, FL, 2002, *SPIE*, Vol. 4728.

[36] S. McGinnity and G. W. Irwin
Multiple model bootstrap filter for maneuvering target tracking.
IEEE Transactions on Aerospace and Electronic Systems, **36** (2000), 1006–1012.

[37] S. McGinnity and G. W. Irwin
Maneuvering target tracking using a multiple-model bootstrap filter.
In A. Doucet, N. de Freitas and N. Gordon (Eds.), *Sequential Monte Carlo Methods in Practice*, Springer, 2001, 479–497.

[38] M. Morelande and S. Challa
Maneuvering target tracking in clutter using particle filters.
IEEE Transactions on Aerospace and Electronic Systems, **41** (2005), 252–270.

[39] D. Mušicki and R. Evans
Clutter map information for data association and track initiation.
IEEE Transactions on Aerospace and Electronic Systems, **40** (2004), 387–398

[40] M. Orton and W. Fitzgerald
A Bayesian approach to tracking multiple targets using sensor arrays and particle filters.
IEEE Transactions on Signal Processing, **50** (2002), 216–223.

[41] M. Orton and A. Marrs
A Bayesian approach to multi-target tracking and data fusion with out-of-sequence measurements.
In *Proceedings of IEE Seminar Target Tracking: Algorithms and Applications*, Oct. 2001, 15/1–15/5.

[42] B. Ristic, S. Arulampalam and N. Gordon
Beyond the Kalman Filter—Particle Filters for Tracking Applications.
Artech House, 2004.

[43] D. B. Rubin
Using the SIR Algorithm to Simulate Posterior Distributions.
Bayesian Statistics, vol. 3, Oxford University Press, 1988, 395–402.

[44] D. J. Salmon and H. Birch
A particle filter for track-before-detect.
In *Proceedings of American Control Conference*, June 2001, 3755–3760.

[45] D. J. Salmond, D. Fisher and N. J. Gordon
Tracking and identification for closely spaced objects in clutter.
In *Proceedings of European Control Conference*, 1997.

[46] D. Schulz, W. Burgard, D. Fox and A. B. Cremers
People tracking with mobile robots using sample-based joint probabilistic data association filters.
The International Journal of Robotics Research, **22** (2003), 99–116.

[47] J. K. Tugnait
Tracking of multiple maneuvering targets in clutter using multiple sensors, IMM and JPDA coupled filtering.
IEEE Transactions on Aerospace and Electronic Systems, **40** (2004), 320–330.

[48] J. Vermaak, S. J. Godsill and P. Perez
Monte Carlo filtering for multi-target tracking and data association.
IEEE Transactions on Aerospace and Electronic Systems, **41** (2005), 309–331.

Henk Blom was born in The Netherlands in 1953. In 1978, he received the M.Sc. degree in electrical engineering from Twente University.

In 1979, he performed research in forward-looking infra-red picture processing at TNO Physics Laboratory, The Hague. In 1980, he joined National Aerospace Laboratory NLR, Amsterdam. In 1988, he was visiting researcher at the University of Connecticut, Storrs, In 1990, he received the Ph.D. degree from Delft University of Technology on a dissertation entitled: "Bayesian Estimation for Decision-Directed Stochastic Control." His research focussed on stochastic hybrid systems with potential applications to air traffic management (ATM), and he gave scientific lead to the development of stochastic analysis based innovative systems in ATM, the most notable of which are ARTAS and TOPAZ. The former is EUROCONTROL's Bayesian multi-sensor multi-target tracking system, which incorporates automated data registration and contingency management. Since 1998, ARTAS has become operational by a steadily increasing number of air traffic control centres within Europe. TOPAZ is NLR's stochastic analysis based accident risk modelling system to provide safety/capacity feedback to advanced ATM designs. Since 2002, TOPAZ has proven its great value in providing safety feedback to the design and introduction of novel ATM operations at Amsterdam Airport. For these innovative system developments he received from NLR the Dr. Ir. B. M. Spee Award in 2004.

Dr. Blom is author or coauthor of over 50 conference papers, 10 journal papers and 10 book chapters, and is coeditor of a Lecture Note in Control and Information Science entitled: "Stochastic Hybrid Systems: Theory and Safety Critical Applications." He is member of joint FAA/Eurocontrol working groups to coordinate future ATM R&D on Separation Minima and on Safety respectively.

Edwin Bloem received the M.Sc. degree in systems and control theory from the University of Twente, Netherlands, in 1993.

Since 1993, he is research engineer at the National Aerospace Laboratory NLR. His work focuses on mathematical modelling for air transport safety and surveillance. His surveillance related work includes the development of advanced tracking algorithms and performance analysis. In the area of air transport safety he has developed extensive models of ATC technical systems and aircraft as well as models for controller and pilot behaviour and their interactions with technical systems. His research interests are in the areas of information fusion, estimation theory, control theory and safety.